ANALYSIS AND APPLICATIONS OF TIME–TRIGGERED STOCHASTIC HYBRID SYSTEM

by

Zikai Xu

A thesis submitted to the Faculty of the University of Delaware in partial fulfillment of the requirements for the degree of Master of Science in Electrical and Computer Engineering

Spring 2019

ANALYSIS AND APPLICATIONS OF TIME–TRIGGERED STOCHASTIC HYBRID SYSTEM

by

Zikai Xu

Approved: _____
Ahbyudai Singh, Ph.D.
Professor in charge of thesis on behalf of the Advisory Committee

Approved: _____
Kenneth E. Barner, Ph.D.
Chair of the Department of Electrical and Computer Engineering

Approved: _____
Levi T. Thompson, Ph.D.
Dean of the College of Engineering

Approved: _____
Douglas J. Doren, Ph.D.
Interim Vice Provost for Graduate and Professional Education

ACKNOWLEDGMENTS

First of all, I would like to thank my advisor Dr. Abhyudai Singh. He gave me lots of help and thoughtful ideas on the way I was writing thesis and doing research. I want to thank my colleagues who have already left the lab Mohammad Soltani and Khem Raj Ghusinga for their collaborations. I am grateful to the Dean, the Faculty, and the Staff of the Department of Electrical and Computer Engineering at the University of Delaware for providing their assistance and support through my M.S. program.

Thanks to my parents Wei and Ling for providing me with support and continuous encouragement throughout my years of studying. I could also thank my friend Jinbo who gave me support and encouragement through my M.S. program. The accomplishment of this thesis would not have been possible without their help. Thank you.

TABLE OF CONTENTS

LIST OF TABLES . . . . . **vi**
LIST OF FIGURES . . . . . **vii**
ABSTRACT . . . . . **x**
NOTATION . . . . . **xi**

Chapter

1 EXACT STATISTICAL MOMENTS OF MULTI-MODE STOCHASTIC HYBRID SYSTEMS WITH RENEWAL TRANSITIONS **1**

1.1 Model Formulation 1
1.2 Statistical Moments of Multi-mode Stochastic Hybrid System 3
1.3 The Steady-State Mean of Multi-mode SHS 4
1.4 The Second-order Moments 7
1.5 Biology Example 9
1.6 Conclusion 12

2 TIME-TRIGGERED STOCHASTIC HYBRID SYSTEM WITH TWO TIMER DEPENDENT RESET **15**

2.1 Model Formulation 16

2.1.1 First family of resets 16

2.1.1.1 The first random reset 18
2.1.1.2 The second random reset 18

2.1.2 Biology Example 19

2.2 Statistical Moments 21

2.2.1 The first-order moment 21

2.2.2 The second-order moments 23

2.3 Biology Example 25

2.3.1 Constant protein synthesis rate 26
2.3.2 Time varying protein synthesis rate 27

2.4 Conclusion 28

3 NOISE ANALYSIS IN BIOCHEMICAL COMPLEX FORMATION 31

3.1 Stochastic Model Formulation 31

3.1.1 Homomer 32
3.1.2 Heteromer 33

3.2 Stochastic Models and Moment Equations 35

3.2.1 Moment Dynamics for Homomer 35
3.2.2 Moment Dynamics for Heteromer 37

3.3 Analysis of Noise Properties of the Complex 37

3.3.1 Steady-State Noise in Homomer level 38
3.3.2 Steady-State Noise in Heteromer level 39

3.4 Conclusion and Future Work 41

BIBLIOGRAPHY 42

LIST OF TABLES

3.1 Description of Stochastic Models for Complex Formation 36

LIST OF FIGURES

1.1 **Schematic of stochastic hybrid systems with two operation modes.** In each mode the states are governed via a set of stochastic differential equations according to (2.1). Resets happen at random times. Any time that an event occurs the states change their value and the system switches to another operation mode. The states after reset depend on the states before reset (eq. 1.4). A timer $\boldsymbol{\tau}$ measures the time since the last even, and rest to zero after each event occurs. 2

1.2 **The fundamental process of gene switching can be modeled through multi-mode framework.** A) Promoter randomly switches between active and inactive states. Protein synthesis only occurs when promoter is ON. Protein is subject to decay with a rate γ. B) The multi-mode system presented here is perfect for modeling promoter toggling. When gene is OFF the protein dynamics are only governed via decay. when promoter becomes active the protein synthesis is modeled through a Langevin equation with a rate k. . 11

1.3 **The noise in protein concentration is highly affected by the gene-switching time intervals.** A) Noise in gene ON time intervals will not change the mean of a protein. Moreover, it does not have an obvious effect on the protein time trend. B) The noise in protein is highly affected by the gene switching noise. While the mean of protein only depends on the ratio of gene ON and OFF times, noise is affected by the magnitude of the ON and OFF time intervals as well. For this plot the protein production rate is selected to be $k = 100$, decay rate is $\gamma = 1\ min^{-1}$, and mean ON and OFF time intervals are equal $\langle \boldsymbol{\tau}_{on} \rangle = \langle \boldsymbol{\tau}_{off} \rangle$. 13

2.1 **Modeling protein concentration in a single cell using time-triggered stochastic hybrid system** *Right*: Protein level $x \in R$ is modeled by SHS with two generally distributed stochastic resets, which are protein synthesis event and cell division event, in a single cell. Cell division time interval is tracked by timer $\boldsymbol{\tau}$; whenever Cell division occurs, the state reset follow (2.16) and timer resets to 0. Additionally, the steady state distribution of protein concentration is simulated by a large number Monte Carlo method. *Left top*: Sketch of mathematical model for protein concentration. Protein concentration is diluted at rate γ. Protein burst size is a random variable $\boldsymbol{u}$. Cell division dose not affect mean of protein concentration. *Left bottom*: zoom-in figure for part of protein concentration evolving with time. 19

2.2 **Deterministic Cell-cycle time affect Fano factor of protein concentration with different protein synthesis rate.** When protein synthesis is a constant, Fano Factor of protein concentration has a monotonically decreasing function with respect to cell-cycle time. The other two protein synthesis rates cause a non-monotonically decreasing function of Fano Factor of protein synthesis. In both cases, an optimal cell-cycle time can be determined to have a minimal Fano Factor value of protein concentration. Fano Factor for protein synthesis $\tau e^{k\tau}$ increase much sharply at long cell-cycle time. Parameters are taken value as: $\langle \boldsymbol{u}^2 \rangle = 2$, $\langle \boldsymbol{u} \rangle = 1\mu g/ml$, $k = 1h^{-1}$, $\gamma = 5\mu g/ml \cdot h^{-1}$, $b = 1$. 30

3.1 **Schematic for complex formation.** *Top:* A species X is produced at a rate k_x and its n_x molecules combine to form a complex (homomer), Z, with rate $f_1(x)$. The species X and the complex Z degrade enzymatically with rates $\gamma_x x$ and $\gamma_z z$ respectively. *Bottom:* Two species, X and Y, are respectively produced at rates k_x and k_y. n_x molecules of X combine with n_y molecules of Y to form a complex (heteromer), Z, with rate $f_2(x, y)$. Both constituting species and the complex decay enzymatically with corresponding rates $\gamma_x x$, $\gamma_y y$ and $\gamma_z z$. 32

3.2 **Noise in complex level as a function of sensitivity of complex formation rate with respect to the species, and relative degradation rates of the complex and the species**. *Top*: The noise in complex level shows a non-monotonic behavior with increase in the sensitivity (normalized by the stoichiometry). The noise further decreases when the stoichiometry of the species in the complex formation process is is higher, suggesting that a higher order multimer can suppress noise better. The noise approaches the Poisson limit of low sensitivity values. *Bottom:*. The non-monotonic curve between noise and sensitivity shifts upwards as the relative degradation rates of the species and the complex are increased. Thus, the noise increases when the complex is relatively unstable than the species. . 39

3.3 **Noise in complex level when complex formation rate has different sensitivities to each constituent**. While the noise behavior shows non-monotonic profile with increase in sensitivity with respect to a constituent, the curve shifts upwards as the sensitivities of both species are changed. This implies that a symmetric sensitivity is better for noise suppression. 40

ABSTRACT

In this paper we provide a new method to derive the exact analytical solutions of the moments for a general class of stochastic hybrid systems. We identified a subclass of stochastic hybrid systems where stochastic resets change the states of the system, and extend our analysis to the systems in which random resets can change both dynamics and the states of system. We provide the exact solutions of first and second order moments. Further, we analyze a class of time-triggered stochastic hybrid systems where the state-space evolves as per a linear time-invariant dynamical system. This continuous time evolution is interspersed with two kinds of stochastic resets. The first reset occurs based on an internal timer that measures the time elapsed since it last occurred. Whenever the first reset occurs the states-space undergoes a random jump and the timer is reset to zero. The second reset occurs based an arbitrary timer-depended rate, and whenever this reset fires, the state-space is changed based on a given random map. For this class of systems, we provide exact conditions that lead to finite statistic moments, and the corresponding exact analytical expressions for the first two moments.

NOTATION

The set of real number is denoted by $\mathbb{R}$. Constant vectors are indicated by a hat, e.g. $\hat{a}$, and matrices are denoted by capital letters. Further, transpose of a matrix A is given by $A^\top$ and the n-dimensional identity matrix is denoted by I_n. We show zero vectors and matrices with the same notation, e.g. $A = \hat{a} = 0$. Random variables are indicated by bold letters. The expected value of a random variable $\boldsymbol{x}$ is denoted by $\langle \boldsymbol{x} \rangle$ and the expected value in steady-state is denoted by $\overline{\langle \boldsymbol{x} \rangle} \equiv \lim_{t\to\infty} \langle \boldsymbol{x} \rangle$. Finally, the conditional expectation of $\boldsymbol{x}$ given another random variable $\boldsymbol{y}$ is denoted $\langle \boldsymbol{x}|_{\boldsymbol{y}} \rangle$.

Chapter 1

EXACT STATISTICAL MOMENTS OF MULTI-MODE STOCHASTIC HYBRID SYSTEMS WITH RENEWAL TRANSITIONS

In this chapeter, we provide a new method to derive the exact analytical solutions of the moments for a general class of stochastic hybrid systems. We previously identified a sub-class of these systems where stochastic resets change the states of the system [53–55]. However, our previous works do not allow that random resets change dynamics of the system. Building on our previous work, here we extend our analysis to the systems in which random resets can change both dynamics and the states of system. We provide the exact solutions of first and second order moments. However, our approach can be generalized to derive any arbitrary moment of these systems (skewness, kurtosis, etc.). We demonstrate our method on an example drawn from systems biology. We quantify noise in protein concentration in the presence of random gene switching times and random synthesis events. We observe that randomness in gene-switching time increases the total noise in protein concentration. Since the noise in gene switching time intervals is a function of the number of steps that needs to be taken before transcription starts, we discuss how noise in protein sheds light on the underlying gene expression mechanisms.

1.1 Model Formulation

The class of systems under study include:

1. **Operation modes**: The system, contains m operative modes. In each mode, the states $\boldsymbol{x} \in \mathbb{R}^{n\times 1}$ are governed via a set of Stochastic Differential Equations (SDEs)

$$d\boldsymbol{x} = (\hat{a}_i + A_i\boldsymbol{x})dt + D_i d\boldsymbol{\omega}_t,\ i = \{1, \ldots, m\}, \tag{1.1}$$

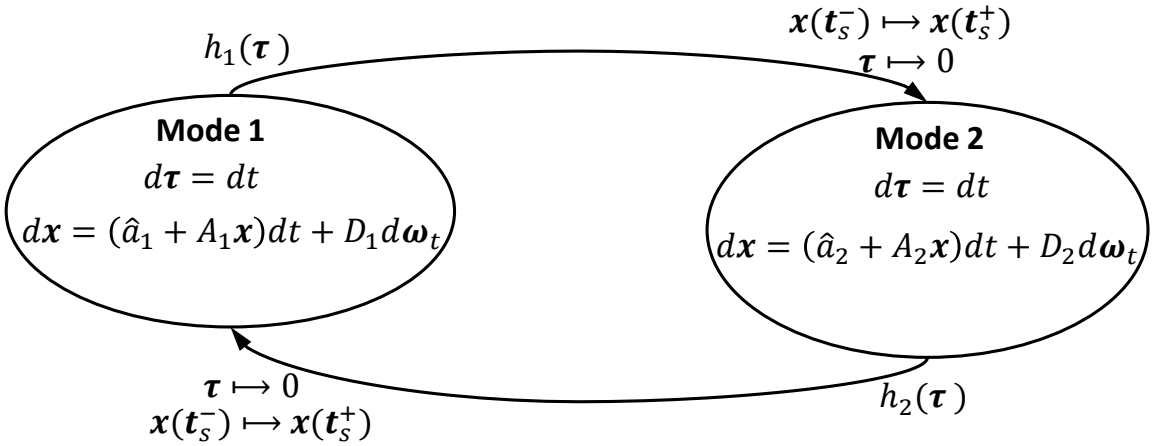

Figure 1.1. Schematic of stochastic hybrid systems with two operation modes. In each mode the states are governed via a set of stochastic differential equations according to (2.1). Resets happen at random times. Any time that an event occurs the states change their value and the system switches to another operation mode. The states after reset depend on the states before reset (eq. 1.4). A timer $\boldsymbol{\tau}$ measures the time since the last even, and rest to zero after each event occurs.

where $A_i \in \mathbb{R}^{n\times n}$, $D_i \in \mathbb{R}^{n\times n}$, and $\hat{a}_i \in \mathbb{R}^{n\times 1}$. Moreover, $\boldsymbol{\omega}_t$ denotes n-dimensional Wiener process where

$$\langle d\boldsymbol{\omega}_t \rangle = 0, \quad \langle d\boldsymbol{\omega}_t d\boldsymbol{\omega}_t^\top \rangle \quad = I_n dt. \tag{1.2}$$

2. **Reset intensity**: When random events occur, the states will change and the system will switch to another mode. Assuming that random events happen at times $\boldsymbol{t}_s$, $s \in \{2, 3, \ldots\}$, the time interval between the events is defined as $\boldsymbol{\tau}_s \equiv \boldsymbol{t}_s - \boldsymbol{t}_{s-1}$. The set of time intervals $\boldsymbol{\tau}_s$ can be divided into m subsets denoting reset time intervals between m different modes. In the rest of this paper for simplicity of notation and mathematical derivations we consider the case of $m = 2$ (Fig. 1). However the obtained results are general and can be applied to any m. In this case system toggles between two modes and $\boldsymbol{\tau}_{s_i}$ is defined as

$$\boldsymbol{\tau}_{s_i} \equiv \boldsymbol{t}_s - \boldsymbol{t}_{s-1} = \begin{cases} i = 1 & \text{from mode 1 to 2,} \\ i = 2 & \text{from mode 2 to 1.} \end{cases} \tag{1.3}$$

3. **Reset maps**: When a reset happens, the states change as

$$\boldsymbol{x}(\boldsymbol{t}_s^-) \mapsto \boldsymbol{x}(\boldsymbol{t}_s^+), \tag{1.4}$$

where $\boldsymbol{x}(\boldsymbol{t}_s^-)$ and $\boldsymbol{x}(\boldsymbol{t}_s^+)$ denote the states of system before and after a reset, respectively. We assume that $\boldsymbol{x}(\boldsymbol{t}_s^+)$ is a random variable in which its expectation is a linear affine map of $\boldsymbol{x}(\boldsymbol{t}_s^-)$. These maps depend on i as

$$\langle \boldsymbol{x}(\boldsymbol{t}_s^+) \rangle = J_i \boldsymbol{x}(\boldsymbol{t}_s^-) + \hat{r}_i, \ i = \{1, 2\}, \tag{1.5}$$

where $J_i \in \mathbb{R}^{n\times n}$ and$\hat{r}_i \in \mathbb{R}^{n\times 1}$. Further, the covariance matrix of $\boldsymbol{x}(\boldsymbol{t}_s^+)$ depends on $\boldsymbol{x}(\boldsymbol{t}_s^-)$ as

$$\begin{aligned}\langle \boldsymbol{x}(\boldsymbol{t}_s^+)\boldsymbol{x}^\top(\boldsymbol{t}_s^+)\rangle - \langle \boldsymbol{x}(\boldsymbol{t}_s^+)\rangle\langle \boldsymbol{x}(\boldsymbol{t}_s^+)\rangle^\top = Q_i\boldsymbol{x}(\boldsymbol{t}_s^-)\boldsymbol{x}^\top(\boldsymbol{t}_s^-)Q_i^\top + B_i\boldsymbol{x}(\boldsymbol{t}_s^-)\hat{c}_i^\top \\ + \hat{c}_i\boldsymbol{x}^\top(\boldsymbol{t}_s^-)B_i^\top + G_i,\ i=\{1,2\}.\end{aligned} \tag{1.6}$$

Here $Q_i \in \mathbb{R}^{n\times n}$, $B_i \in \mathbb{R}^{n\times n}$,$G_i \in \mathbb{R}^{n\times n}$, and $\hat{c}_i \in \mathbb{R}^{n\times 1}$. In previous studies, we showed that the matrices Q_i, B_i, C_i, and G_i can be used to model presence of constant or state-dependent noise in $\boldsymbol{x}$ [6, 49, 51, 52, 60].

1.2 Statistical Moments of Multi-mode Stochastic Hybrid System

In order to obtain a mathematically tractable model, we introduce a timer $\boldsymbol{\tau}$ that measures the time since the last event. The timer increases with time between the events

$$d\boldsymbol{\tau} = dt, \tag{1.7}$$

and resets to zero whenever a new event occurs

$$\boldsymbol{\tau} \mapsto 0. \tag{1.8}$$

Note that we have two modes in the system, and the time intervals that the system resides in each of them is independent from the other. Thus we further divide set of $\boldsymbol{\tau}$ into two subsets $\boldsymbol{\tau}_1$ and $\boldsymbol{\tau}_2$ indicating the accumulation of time in mode 1 and 2, respectively ($\boldsymbol{\tau} = \{\boldsymbol{\tau}_1, \boldsymbol{\tau}_2\}$).

With this definition we can connect the probability of occurrence of an event to probability density function of the time intervals between the events. Let the probability that a transmission occurs in the next infinitesimal time $(t, t+dt]$ be $h_i(\boldsymbol{\tau})dt$, where

$$h_i(\tau) \equiv \frac{f_i(\tau)}{1-\int_{y=0}^{\tau} f_i(y)dy},\ i=\{1,2\}, \tag{1.9}$$

Then, the time interval between events $\boldsymbol{\tau}_{s_i}$ follows a probability density function f_i

$$\boldsymbol{\tau}_{s_i} \sim f_i(\tau) = h_i(\tau)e^{-\int_{y=0}^{\tau} f_i(y)dy}, i=\{1,2\} \tag{1.10}$$

[13, 35, 41], and timers follow the following density function [60]

$$\boldsymbol{\tau}_i \sim p_i(\tau) = \frac{1}{\langle \boldsymbol{\tau}_{s_i}\rangle} e^{-\int_{y=0}^{\tau} f_i(y)dy},\ i=\{1,2\}. \tag{1.11}$$

Finally, note that the probability that the system resides in each mode is independent of the states of system and is given by

$$\begin{aligned}\text{Probability of being in mode 1} &= \frac{\langle \boldsymbol{\tau}_{s_1} \rangle}{\langle \boldsymbol{\tau}_{s_1} \rangle + \langle \boldsymbol{\tau}_{s_2} \rangle},\\ \text{Probability of being in mode 2} &= \frac{\langle \boldsymbol{\tau}_{s_2} \rangle}{\langle \boldsymbol{\tau}_{s_1} \rangle + \langle \boldsymbol{\tau}_{s_2} \rangle}.\end{aligned} \tag{1.12}$$

1.3 The Steady-State Mean of Multi-mode SHS

By introducing the timer, we can derive the steady-state mean of $\boldsymbol{x}$ in the following theorem.

Theorem 1 *The steady-state mean of states of stochastic hybrid system in* (2.1)-(1.6) *is given by* (1.13)

$$\begin{aligned}\overline{\langle \boldsymbol{x} \rangle} = &\frac{\langle \boldsymbol{\tau}_{s_1} \rangle}{\langle \boldsymbol{\tau}_{s_1} \rangle + \langle \boldsymbol{\tau}_{s_2} \rangle} \Big(\langle e^{A_1 \boldsymbol{\tau}_1} \rangle (I_n - J_2 \langle e^{A_2 \boldsymbol{\tau}_{s_2}} \rangle J_1 \langle e^{A_1 \boldsymbol{\tau}_{s_1}} \rangle)^{-1} \Big(J_2 \langle e^{A_2 \boldsymbol{\tau}_{s_2}} \rangle \Big\langle e^{A_1 \boldsymbol{\tau}_{s_1}} \int_0^{\boldsymbol{\tau}_{s_1}} e^{-A_1 l} \hat{a}_1 dl \Big\rangle + J_2 \langle e^{A_2 \boldsymbol{\tau}_{s_2}} \rangle \hat{r}_1 \\ &+ \Big\langle e^{A_2 \boldsymbol{\tau}_{s_2}} \int_0^{\boldsymbol{\tau}_{s_2}} e^{-A_2 l} \hat{a}_2 dl \Big\rangle + \hat{r}_2 \Big) + \Big\langle e^{A_1 \boldsymbol{\tau}_1} \int_0^{\boldsymbol{\tau}_1} e^{-A_1 l} \hat{a}_1 dl \Big\rangle \Big) \\ &+ \frac{\langle \boldsymbol{\tau}_{s_2} \rangle}{\langle \boldsymbol{\tau}_{s_1} \rangle + \langle \boldsymbol{\tau}_{s_2} \rangle} \Big(\langle e^{A_2 \boldsymbol{\tau}_2} \rangle \Big(I_n - J_1 \langle e^{A_1 \boldsymbol{\tau}_{s_1}} \rangle J_2 \langle e^{A_2 \boldsymbol{\tau}_{s_2}} \rangle)^{-1} (J_1 \langle e^{A_1 \boldsymbol{\tau}_{s_1}} \rangle \Big\langle e^{A_2 \boldsymbol{\tau}_{s_2}} \int_0^{\boldsymbol{\tau}_{s_2}} e^{-A_2 l} \hat{a}_2 dl \Big\rangle + J_1 \langle e^{A_1 \boldsymbol{\tau}_{s_1}} \rangle \hat{r}_2 \\ &+ \Big\langle e^{A_1 \boldsymbol{\tau}_{s_1}} \int_0^{\boldsymbol{\tau}_{s_1}} e^{-A_1 l} \hat{a}_1 dl \Big\rangle + \hat{r}_1 \Big) + \Big\langle e^{A_2 \boldsymbol{\tau}_2} \int_0^{\boldsymbol{\tau}_2} e^{-A_2 l} \hat{a}_2 dl \Big\rangle \Big).\end{aligned} \tag{1.13}$$

if and only if

$$\langle e^{A_i \boldsymbol{\tau}_{s_i}} \rangle = \int_0^\infty f_i(\tau) e^{-A_i \tau} d\tau, \ \ i = \{1, 2\} \tag{1.14}$$

is finite, and all the eigenvalues of the matrices $J_2 \langle e^{A_2 \boldsymbol{\tau}_{s_2}} \rangle J_1 \langle e^{A_1 \boldsymbol{\tau}_{s_1}} \rangle$ *and* $J_1 \langle e^{A_1 \boldsymbol{\tau}_{s_1}} \rangle J_2 \langle e^{A_2 \boldsymbol{\tau}_{s_2}} \rangle$ *are inside unit circle.*

■

Proof of theorem 1 consists of two parts, we start with assuming that the system is residing in mode 1, hence the states of the system right before the s^{th} event is

$$\boldsymbol{x}(\boldsymbol{t}_s^-) = e^{A_1 \boldsymbol{\tau}_{s_1}} \boldsymbol{x}(\boldsymbol{t}_{s-1}^+) + \int_0^{\boldsymbol{\tau}_{s_1}} e^{-A_1 l} \hat{a}_1 dl + \int_0^{\boldsymbol{\tau}_{s_1}} D_1 d\omega_t. \tag{1.15}$$

By using (1.5), the mean of the states after the s^{th} event is

$$\langle \boldsymbol{x}(\boldsymbol{t}_s^+) \rangle = J_1 (\langle e^{A_1 \boldsymbol{\tau}_{s_1}} \rangle \langle \boldsymbol{x}(\boldsymbol{t}_{s-1}^+) \rangle + \Big\langle e^{A_1 \boldsymbol{\tau}_{s_1}} \int_0^{\boldsymbol{\tau}_{s_1}} e^{-A_1 l} \hat{a}_1 dl \Big\rangle) + \hat{r}_1. \tag{1.16}$$

After the s^{th} event the system is residing in mode 2. Hence the states of the system before $s+1^{th}$ event is given by

$$\boldsymbol{x}(\boldsymbol{t}_{s+1}^{-}) = e^{A_2\boldsymbol{\tau}_{s_2}}\boldsymbol{x}(\boldsymbol{t}_s^{+}) + \int_0^{\boldsymbol{\tau}_{s_2}} e^{-A_2 l}\hat{a}_2 dl + \int_0^{\boldsymbol{\tau}_{s_2}} D_2 d\omega_t. \tag{1.17}$$

Again by using (1.5) we derive the values of states right after $s+1^{th}$ event

$$\langle \boldsymbol{x}(\boldsymbol{t}_{s+1}^{+})\rangle = J_2(\left\langle e^{A_2\boldsymbol{\tau}_{s_2}}\right\rangle \left\langle \boldsymbol{x}(\boldsymbol{t}_s^{+})\right\rangle + \left\langle e^{A_2\boldsymbol{\tau}_{s_2}} \int_0^{\boldsymbol{\tau}_{s_2}} e^{-A_2 l}\hat{a}_2 dl \right\rangle) + \hat{r}_2. \tag{1.18}$$

Substituting (1.16) into (1.18), we get

$$\begin{aligned}\langle \boldsymbol{x}(\boldsymbol{t}_{s+1}^{+})\rangle &= J_2\langle e^{A_2\boldsymbol{\tau}_{s_2}}\rangle J_1\langle e^{A_1\boldsymbol{\tau}_{s_1}}\rangle \left\langle \boldsymbol{x}(\boldsymbol{t}_{s-1}^{+})\right\rangle + J_2\langle e^{A_2\boldsymbol{\tau}_{s_2}}\rangle \left\langle e^{A_1\boldsymbol{\tau}_{s_1}} \int_0^{\boldsymbol{\tau}_{s_1}} e^{-A_1 l}\hat{a}_1 dl \right\rangle \\ &+ J_2\langle e^{A_2\boldsymbol{\tau}_{s_2}}\rangle \hat{r}_1 + \left\langle e^{A_2\boldsymbol{\tau}_{s_2}} \int_0^{\boldsymbol{\tau}_{s_2}} e^{-A_2 l}\hat{a}_2 dl \right\rangle + \hat{r}_2.\end{aligned} \tag{1.19}$$

Note that after $s+1^{th}$ event we have returned to mode 1. Hence in order to have a finite recursive equation, all the eigenvalues of $J_2\langle e^{A_2\boldsymbol{\tau}_{s_2}}\rangle J_1\langle e^{A_1\boldsymbol{\tau}_{s_1}}\rangle$ should be inside the unit circle. In this limit, the mean of states right after returning to mode 1 in steady-state is

$$\begin{aligned}\overline{\langle \boldsymbol{x}(\boldsymbol{t}_s^{+})\rangle} &= V_1 J_2\langle e^{A_2\boldsymbol{\tau}_{s_2}}\rangle \left\langle e^{A_1\boldsymbol{\tau}_{s_1}} \int_0^{\boldsymbol{\tau}_{s_1}} e^{-A_1 l}\hat{a}_1 dl \right\rangle + V_1 J_2\langle e^{A_2\boldsymbol{\tau}_{s_2}}\rangle \hat{r}_1 \\ &+ V_1 \left\langle e^{A_2\boldsymbol{\tau}_{s_2}} \int_0^{\boldsymbol{\tau}_{s_2}} e^{-A_2 l}\hat{a}_2 dl \right\rangle + V_1 \hat{r}_2,\end{aligned} \tag{1.20}$$

where

$$V_1 = (I_n - J_2\langle e^{A_2\boldsymbol{\tau}_{s_2}}\rangle J_1\langle e^{A_1\boldsymbol{\tau}_{s_1}}\rangle)^{-1}. \tag{1.21}$$

By having the steady state initial condition of being in mode 1, we can calculate the mean of states for any time $\boldsymbol{\tau}_1 = \tau$

$$\begin{aligned}\overline{\langle \boldsymbol{x}|_{\boldsymbol{\tau}_1=\tau}\rangle} &= e^{A_1\tau} \int_0^{\tau} e^{-A_1 l}\hat{a}_1 dl + e^{A_1\tau} V_1 (J_2 \left\langle e^{A_2\boldsymbol{\tau}_{s_2}}\right\rangle \left\langle e^{A_1\boldsymbol{\tau}_{s_1}} \int_0^{\boldsymbol{\tau}_{s_1}} e^{-A_1 l}\hat{a}_1 dl \right\rangle \\ &+ J_2 \left\langle e^{A_2\boldsymbol{\tau}_{s_2}}\right\rangle \hat{r}_1 + \left\langle e^{A_2\boldsymbol{\tau}_{s_2}} \int_0^{\boldsymbol{\tau}_{s_2}} e^{-A_2 l}\hat{a}_2 dl \right\rangle + \hat{r}_2).\end{aligned} \tag{1.22}$$

In the next part, we repeat our analysis by assuming that system is residing in mode 2. Such analysis results in another recursive formula which is converging if all the eigenvalues of $J_1\langle e^{A_1\boldsymbol{\tau}_{s_1}}\rangle J_2\langle e^{A_2\boldsymbol{\tau}_{s_2}}\rangle$ are inside the unit circle. In this case we can calculate the steady-state mean of states for any time $\boldsymbol{\tau}_2 = \tau$ as

$$\begin{aligned}\overline{\langle \boldsymbol{x}|_{\boldsymbol{\tau_2}=\tau}\rangle} = e^{A_2\tau}\int_0^{\tau} e^{-A_2 l}\hat{a}_2 dl e^{A_2\tau} V_2(J_1\left\langle e^{A_1\boldsymbol{\tau}_{s_1}}\right\rangle\left\langle e^{A_2\boldsymbol{\tau}_{s_2}}\int_0^{\boldsymbol{\tau}_{s_2}} e^{-A_2 l}\hat{a}_2 dl\right\rangle \\ + J_1\left\langle e^{A_1\boldsymbol{\tau}_{s_1}}\right\rangle\hat{r}_2 + \left\langle e^{A_1\boldsymbol{\tau}_{s_1}}\int_0^{\boldsymbol{\tau}_{s_1}} e^{-A_1 l}\hat{a}_1 dl\right\rangle + \hat{r}_1),\end{aligned} \tag{1.23}$$

where

$$V_2 = (I_n - J_1\langle e^{A_1\boldsymbol{\tau}_{s_1}}\rangle J_2\langle e^{A_2\boldsymbol{\tau}_{s_2}}\rangle)^{-1}. \tag{1.24}$$

Moreover, note that

$$\begin{aligned}A\left\langle e^{A_i\boldsymbol{\tau}_{s_i}}\int_0^{\boldsymbol{\tau}_{s_i}} e^{-A_i l}\hat{a}_i dl\right\rangle &= A\int_0^{\infty} f_i(\tau)(e^{-A_i\tau_i}\int_0^{\boldsymbol{\tau}_i} e^{-A_i l}\hat{a}_i dl)d \\ &= \int_0^{\infty} f_i(\tau)e^{-A_i\tau_i}(I - e^{-A_i\tau_i})\hat{a}_i d\tau = -(I_n - \langle e^{A_i\boldsymbol{\tau}_{s_i}}\rangle)\hat{a}_i,\end{aligned} \tag{1.25}$$

and

$$\begin{aligned}\langle e^{A_i\boldsymbol{\tau}_{s_i}}\rangle &= \int_0^{\infty} h_i(\tau)e^{-\int_0^{\tau_i} h_i(y)dy}e^{A_i\tau}d\tau \\ &= (-e^{-\int_0^{\tau} h_i(y)dy}e^{A_i\tau_i})_0^{\infty} + \int_0^{\infty} e^{-\int_0^{\tau_i} h_i(y)dy}e^{A_i\tau}A_i d\tau \\ &= I_n + \langle\boldsymbol{\tau}_{s_i}\rangle\langle e^{A_i\boldsymbol{\tau}_i}\rangle A_i.\end{aligned} \tag{1.26}$$

Hence if $\langle e^{A_i\boldsymbol{\tau}_{s_i}}\rangle$ exists then $\langle e^{A_i\boldsymbol{\tau}_i}\int_0^{\boldsymbol{\tau}_i} e^{-A_i l}\hat{a}_i dl\rangle$ and $\langle e^{A_i\boldsymbol{\tau}_i}\rangle$ are also finite. Finally, taking expected value with respect to $\boldsymbol{\tau}_i$, $i = \{1, 2\}$ from (1.22) and (1.23) by using (2.6) and then using (1.12) results in (1.13) and that completes our proof.

In general, matrices cannot commute, thus, $J_2\langle e^{A_2\boldsymbol{\tau}_{s_2}}\rangle J_1\langle e^{A_1\boldsymbol{\tau}_{s_1}}\rangle$ is not equal to $J_1\langle e^{A_1\boldsymbol{\tau}_{s_1}}\rangle J_2\langle e^{A_2\boldsymbol{\tau}_{s_2}}\rangle$. This implies an important property of these systems: even if each mode is stable, it does not result in stability of the whole system. Note that the states of the system at a given time depends on the entire history of the resets.

1.4 The Second-order Moments

In [54] we introduced a method to convert dynamics of the second-order moments to a similar form as in (2.1) and (1.4). This is done by introducing a new vector

$$\boldsymbol{\mu} \equiv [\boldsymbol{x}^\top \ \mathrm{vec}(\boldsymbol{x}\boldsymbol{x}^\top)^\top]^\top, \tag{1.27}$$

where $\mathrm{vec}(\boldsymbol{x}\boldsymbol{x}^\top) \in \mathbb{R}^{n^2\times 1}$ stands for vector representation of the matrix $\boldsymbol{x}\boldsymbol{x}^\top \in \mathbb{R}^{n\times n}$. The values of $\boldsymbol{x}\boldsymbol{x}^\top$ after a reset is given by (1.6), and we need to derive its dynamics in between the events. From (2.1) and Ito formula [27], it follows that

$$d(\boldsymbol{x}\boldsymbol{x}^\top) = \left(A_i\boldsymbol{x}\boldsymbol{x}^\top + \boldsymbol{x}\boldsymbol{x}^\top A_i^\top + \hat{a}_i\boldsymbol{x}^\top + \boldsymbol{x}\hat{a}_i^\top + D_iD_i^\top\right) dt, \tag{1.28}$$

$i = \{1, 2\}$. Using vectorization on this equation results in

$$\begin{aligned} d\mathrm{vec}\left(\boldsymbol{x}\boldsymbol{x}^\top\right) = \big((I_n \otimes A_i + A_i \otimes I_n)\,\mathrm{vec}\left(\boldsymbol{x}\boldsymbol{x}^\top\right) \\ +\mathrm{vec}\left(D_iD_i^\top\right) + (I_n \otimes \hat{a}_i + \hat{a}_i \otimes I_n)\boldsymbol{x})\big)\, dt, i = \{1, 2\} \end{aligned} \tag{1.29}$$

[32]. From (2.1) and (2.32), the dynamics of $\boldsymbol{\mu}$ between the events is given by

$$d\boldsymbol{\mu} = (\hat{a}_{\mu_i} + A_{\mu_i}\boldsymbol{\mu}(t))dt + (C_{\mu_i})d\boldsymbol{w}_t, \tag{1.30}$$

where

$$\begin{aligned} A_{\mu_i} &= \left[\begin{array}{c|c} A_i & 0 \\ \hline I_n \otimes \hat{a}_i + \hat{a}_i \otimes I_n & I_n \otimes A_i + A_i \otimes I_n \end{array}\right], \\ \hat{a}_{\mu_i} &= \left[\begin{array}{c} \hat{a}_i \\ \hline \mathrm{vec}\left(D_iD_i^\top\right) \end{array}\right]. \end{aligned} \tag{1.31}$$

Note that we did not show C_{μ_i} because this matrix has no role in the steady-state mean of $\boldsymbol{\mu}$ [27].

Moreover, when a reset occurs, the states of $\boldsymbol{\mu}$ reset as

$$\boldsymbol{\mu}(\boldsymbol{t}_s^-) \mapsto \boldsymbol{\mu}(\boldsymbol{t}_s^+), \tag{1.32}$$

where

$$\langle \boldsymbol{\mu}(\boldsymbol{t}_s^+)\rangle = J_{\mu_i}\boldsymbol{\mu}(\boldsymbol{t}_s^-) + \hat{r}_{\mu_i}, \tag{1.33a}$$

$$J_{\mu_i} = \left[\begin{array}{c:c} J_i & 0 \\ \hdashline M_i & N_i \end{array}\right], \hat{r}_{\mu_i} = \left[\begin{array}{c} \hat{r}_i \\ \hdashline \mathrm{vec}\left(G_i G_i^\top\right) \end{array}\right], \tag{1.33b}$$

$$M_i = B_i \otimes \hat{c}_i + \hat{c}_i \otimes B_i + J_i \otimes \hat{r}_i + \hat{r}_i \otimes J_i,$$

$$N_i = J_i \otimes J_i + Q_i \otimes Q_i.$$

Deterministic dynamics (2.32) and stochastic resets (1.32) are similar to (2.1) and (1.4). Hence with a similar analysis as in Theorem 1, the following theorem provides the necessary and sufficient conditions for having the steady-state second-order moments of $\boldsymbol{x}$.

Theorem 2 *Suppose that the multi-mode stochastic hybrid system in (2.1)-(1.6) satisfies the hypothesis of Theorem 1, then the steady-state mean of $\boldsymbol{x}\boldsymbol{x}^\top$ is finite if and only if all the eigenvalues of the matrices*

1. $(J_2 \otimes J_2 + Q_2 \otimes Q_2)\langle e^{A_2\boldsymbol{\tau}_{s_2}} \otimes e^{A_2\boldsymbol{\tau}_{s_2}}\rangle (J_1 \otimes J_1 + Q_1 \otimes Q_1)\langle e^{A_1\boldsymbol{\tau}_{s_1}} \otimes e^{A_1\boldsymbol{\tau}_{s_1}}\rangle$,
2. $(J_1 \otimes J_1 + Q_1 \otimes Q_1)\langle e^{A_1\boldsymbol{\tau}_{s_1}} \otimes e^{A_1\boldsymbol{\tau}_{s_1}}\rangle (J_2 \otimes J_2 + Q_2 \otimes Q_2)\langle e^{A_2\boldsymbol{\tau}_{s_2}} \otimes e^{A_2\boldsymbol{\tau}_{s_2}}\rangle$

are inside the unite circle.

■

First let us define

$$\boldsymbol{y}_i \equiv e^{A_i\boldsymbol{\tau}_{s_i}} \int_0^{\boldsymbol{\tau}_{s_i}} e^{-A_i l}\hat{a}_i dl. \tag{1.34}$$

Similar to Theorem 1 we prove Theorem 2 in two parts. Assume that system is residing in mode 1, then $\boldsymbol{x}\boldsymbol{x}^\top$ right after s^{th} event is related to $\boldsymbol{x}(\boldsymbol{t}_{s-1}^+)\boldsymbol{x}^\top(\boldsymbol{t}_{s-1}^+)$ as

$$\begin{aligned}
\mathrm{vec}(\langle \boldsymbol{x}(\boldsymbol{t}_s^+)\boldsymbol{x}^\top(\boldsymbol{t}_s^+)\rangle) &= (J_1 \otimes J_1 + Q_1 \otimes Q_1)\langle e^{A_1\boldsymbol{\tau}_{s_1}} \otimes e^{A_1\boldsymbol{\tau}_{s_1}}\rangle \mathrm{vec}(\langle \boldsymbol{x}(\boldsymbol{t}_{s-1}^+)\boldsymbol{x}^\top(\boldsymbol{t}_{s-1}^+)\rangle \\
&+ (J_1 \otimes J_1 + Q_1 \otimes Q_1)(\langle e^{A_1\boldsymbol{\tau}_{s_1}} \otimes \boldsymbol{y}_1\rangle\langle \boldsymbol{y}_1 \otimes e^{A_1\boldsymbol{\tau}_{s_1}}\rangle)\langle \boldsymbol{x}(\boldsymbol{t}_{s-1}^+)\rangle \\
&+ ((B_1 \otimes \hat{c}_1 + J_1 \otimes \hat{r}_1)\langle I_n \otimes e^{A_1\boldsymbol{\tau}_{s_1}}\rangle \\
&+ (\hat{c}_1 \otimes B_1 + \hat{r}_1 \otimes J_1)\langle e^{A_1\boldsymbol{\tau}_{s_1}} \otimes I_n\rangle)\langle \boldsymbol{x}(\boldsymbol{t}_{s-1}^+)\rangle \\
&+ \mathrm{vec}(Q_1 \left\langle \boldsymbol{y}_1\boldsymbol{y}_1{}^\top \right\rangle Q_1^\top + J_1 \left\langle \boldsymbol{y}_1\boldsymbol{y}_1{}^\top \right\rangle J_1^\top + B_1 \langle \boldsymbol{y}_1\rangle \hat{c}_1{}^\top \\
&+ J_1 \langle \boldsymbol{y}_1\rangle \hat{r}_1{}^\top + \hat{c}_1 \left\langle \boldsymbol{y}_1{}^\top \right\rangle B_1^\top + \hat{r}_1 \left\langle \boldsymbol{y}_1{}^\top \right\rangle J_1^\top + G_1 + \hat{r}_1\hat{r}_1{}^\top).
\end{aligned} \tag{1.35}$$

Next, $\boldsymbol{x}\boldsymbol{x}^\top$ right after $s+1^{th}$ event is related to $\boldsymbol{x}(\boldsymbol{t}_s^+)\boldsymbol{x}^\top(\boldsymbol{t}_s^+)$ as

$$\begin{aligned}\mathrm{vec}(\langle \boldsymbol{x}(\boldsymbol{t}_{s+1}^+)\boldsymbol{x}^\top(\boldsymbol{t}_{s+1}^+)\rangle) &= (J_2\otimes J_2+Q_2\otimes Q_2)\langle e^{A_2\boldsymbol{\tau}_{s_2}}\otimes e^{A_2\boldsymbol{\tau}_{s_2}}\rangle \mathrm{vec}(\langle \boldsymbol{x}(\boldsymbol{t}_s^+)\boldsymbol{x}^\top(\boldsymbol{t}_s^+)\rangle \\ &+ (J_2\otimes J_2+Q_2\otimes Q_2)(\langle e^{A_2\boldsymbol{\tau}_{s_2}}\otimes \boldsymbol{y}_2\rangle + \langle \boldsymbol{y}_2\otimes e^{A_2\boldsymbol{\tau}_{s_2}}\rangle)\langle \boldsymbol{x}(\boldsymbol{t}_s^+)\rangle \\ &+ ((B_2\otimes \hat{c_2}+J_2\otimes \hat{r_2})\langle I_n\otimes e^{A_2\boldsymbol{\tau}_{s_2}}\rangle \\ &+ (\hat{c_2}\otimes B_2+\hat{r_2}\otimes J_2)\langle e^{A_2\boldsymbol{\tau}_{s_2}}\otimes I_n\rangle)\langle \boldsymbol{x}(\boldsymbol{t}_s^+)\rangle \\ &+ \mathrm{vec}(Q_2\left\langle \boldsymbol{y}_2\boldsymbol{y}_2{}^\top\right\rangle Q_2^\top + J_2\left\langle \boldsymbol{y}_2\boldsymbol{y}_2{}^\top\right\rangle J_2^\top + B_2\langle \boldsymbol{y}_2\rangle \hat{c_2}{}^\top \\ &+ J_2\langle \boldsymbol{y}_2\rangle \hat{r_2}{}^\top + \hat{c_2}\left\langle \boldsymbol{y}_2{}^\top\right\rangle B_2^\top + \hat{r_2}\left\langle \boldsymbol{y}_2{}^\top\right\rangle J_2^\top + G_2 + \hat{r_2}\hat{r_2}{}^\top).\end{aligned} \tag{1.36}$$

Combining these two equations we obtain a recursive formula in which is converging in steady-state if all the eigenvalues of $(J_2\otimes J_2+Q_2\otimes Q_2)\langle e^{A_2\boldsymbol{\tau}_{s_2}}\otimes e^{A_2\boldsymbol{\tau}_{s_2}}\rangle(J_1\otimes J_1+Q_1\otimes Q_1)\langle e^{A_1\boldsymbol{\tau}_{s_1}}\otimes e^{A_1\boldsymbol{\tau}_{s_1}}\rangle$ are inside unit circle. Similarly if we assume that the system resides in mode 2 then the steady-state values exists if all the eigenvalues of $(J_1\otimes J_1+Q_1\otimes Q_1)\langle e^{A_1\boldsymbol{\tau}_{s_1}}\otimes e^{A_1\boldsymbol{\tau}_{s_1}}\rangle(J_2\otimes J_2+Q_2\otimes Q_2)\langle e^{A_2\boldsymbol{\tau}_{s_2}}\otimes e^{A_2\boldsymbol{\tau}_{s_2}}\rangle$ are inside the unit circle. The rest of proof is similar to that of Theorem 1.

Please see Appendix B for detailed derivations. Finally, $\overline{\langle \boldsymbol{\mu}\boldsymbol{\mu}^\top\rangle}$ can be obtained from (1.13) by replacing A_i, $\hat{a}_i$, J_i, and $\hat{r}_i$ in (1.13) with their respective A_{μ_i}, $\hat{a}_{\mu_i}$, J_{μ_i}, and $\hat{r}_{\mu_i}$, $i=\{1,2\}$. In the next section, we apply our results on a biological example.

1.5 Biology Example

Inside a living cell different species show considerable levels of fluctuations (noise) even between isogenic cells in an identical environment [4,38,40]. These fluctuations may have beneficial or harmful effects such as corrupting functioning of gene networks [1,12,31] or helping cells to survive in an ever changing environment [5,11,29,61].

A main source of noise is occurrence of random events such as protein synthesis, binding, etc. [7,33,39]. One such important event is stochastic gene switching: a gene becomes active for a short period of time followed by a period of silence [9,25,42,43,47,62].

To explore the contribution of gene switching on protein concentration, we used the multi-mode stochastic hybrid system introduced in the previous section. Let $\boldsymbol{x}(t)$

denotes a protein concentration level inside the cell at time t. We assume that production occurs in exponentially distributed time intervals with rate k and we use a Langevin approximation of this reaction [22]. Further we consider that protein decays with a rate γ. When gene is active, the dynamics of protein concentration can be written as

$$d\boldsymbol{x} = (k - \gamma \boldsymbol{x})dt + \sqrt{k}\, d\boldsymbol{w}_t, \tag{1.37}$$

and when gene is inactive, protein dynamics only include decay

$$d\boldsymbol{x} = -\gamma \boldsymbol{x} dt. \tag{1.38}$$

Note that decay of protein concentration is mainly caused by cell growth. Since cell growth is a cellular process which is the summation of many random events, we did not consider any noise in the decay of proteins [3, 20, 60]. The dynamics of this system are in the form of (2.1) with

$$A_1 = A_2 = -\gamma,\ \hat{a}_1 = k,\ D_1 = \sqrt{k},\ \hat{a}_2 = 0,\ D_2 = 0. \tag{1.39}$$

Moreover, $J_1 = J_2 = 1$, and $\hat{r}_i = Q_i = B_i = G_i = \hat{c}_i = 0,\ i = \{1, 2\}$ (Fig. 2). For having a clear connection to our biological example, we rename $\boldsymbol{\tau}_{s_1}$ and $\boldsymbol{\tau}_{s_2}$ as $\boldsymbol{\tau}_{on}$ and $\boldsymbol{\tau}_{off}$, respectively.

Since $A_1 = A_2 = -\gamma < 0$, then both $\langle e^{-\gamma \boldsymbol{\tau}_{off}} \rangle$ and $\langle e^{-\gamma \boldsymbol{\tau}_{on}} \rangle$ exist. Moreover, because $J_1 = J_2 = 1$ then $\langle e^{-\gamma \boldsymbol{\tau}_{off}} \rangle \langle e^{-\gamma \boldsymbol{\tau}_{on}} \rangle < 1$, hence we can use (1.13) to derive the steady-state mean of protein concentration

$$\overline{\langle \boldsymbol{x} \rangle} = \frac{\langle \boldsymbol{\tau}_{on} \rangle}{\langle \boldsymbol{\tau}_{on} \rangle + \langle \boldsymbol{\tau}_{off} \rangle} \frac{k}{\gamma}. \tag{1.40}$$

The mean of protein concentration is independent of the probability density function of gene-switching time intervals. This means that the mean of protein contains no information about the underlying processes that leads to gene activation.

In the next step, we derive the second-order moment of protein to explore how variations in gene-switching time intervals affect the fluctuations in protein count.

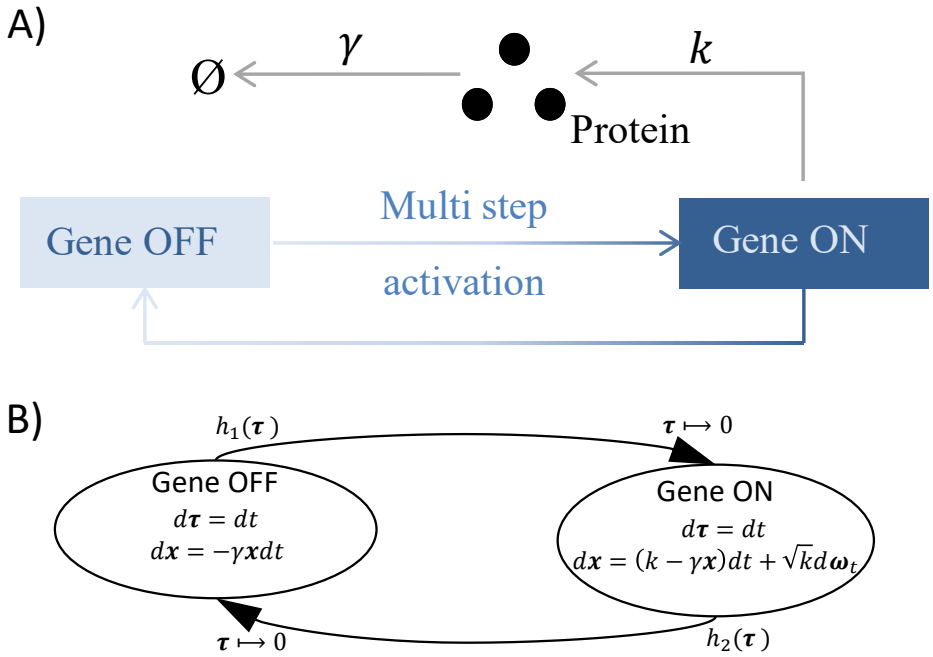

Figure 1.2. The fundamental process of gene switching can be modeled through multi-mode framework. A) Promoter randomly switches between active and inactive states. Protein synthesis only occurs when promoter is ON. Protein is subject to decay with a rate γ. B) The multi-mode system presented here is perfect for modeling promoter toggling. When gene is OFF the protein dynamics are only governed via decay. when promoter becomes active the protein synthesis is modeled through a Langevin equation with a rate k.

First, we use (1.31) to derive the matrices needed for calculating the second-order moment

$$A_{\mu_1} = \begin{bmatrix} -\gamma & 0 \\ 0 & -2\gamma \end{bmatrix}, \hat{a}_{\mu_1} = \begin{bmatrix} k \\ k \end{bmatrix}, A_{\mu_2} = \begin{bmatrix} -\gamma & 0 \\ 2k & -2\gamma \end{bmatrix}, \tag{1.41}$$
$$\hat{a}_{\mu_2} = 0, J_{\mu_1} = J_{\mu_2} = I_2.$$

Further, here $J_{\mu_i} = I_2$ and $\hat{r}_{\mu_i} = 0,\ i = \{1, 2\}$. Since $-\gamma < 0$ then the conditions of Theorem 2 are satisfied and we can derive the second-order moment as

$$\begin{aligned} \overline{\langle \boldsymbol{x}^2 \rangle} = & \frac{k^2}{\gamma^3} \frac{(\langle e^{-\gamma \boldsymbol{\tau}_{off}} \rangle - 1)(\langle e^{-\gamma \boldsymbol{\tau}_{on}} \rangle - 1)}{(\langle e^{-\gamma \boldsymbol{\tau}_{off}} \rangle \langle e^{-\gamma \boldsymbol{\tau}_{on}} \rangle - 1)(\langle \boldsymbol{\tau}_{on} \rangle + \langle \boldsymbol{\tau}_{off} \rangle)} \\ & + \frac{k^2}{\gamma^2} \frac{(\langle e^{-\gamma \boldsymbol{\tau}_{off}} \rangle \langle e^{-\gamma \boldsymbol{\tau}_{on}} \rangle - 1)\langle \boldsymbol{\tau}_{on} \rangle}{(\langle e^{-\gamma \boldsymbol{\tau}_{off}} \rangle \langle e^{-\gamma \boldsymbol{\tau}_{on}} \rangle - 1)(\langle \boldsymbol{\tau}_{on} \rangle + \langle \boldsymbol{\tau}_{off} \rangle)} \\ & + \frac{k}{2\gamma} \frac{\langle \boldsymbol{\tau}_{on} \rangle}{\langle \boldsymbol{\tau}_{on} \rangle + \langle \boldsymbol{\tau}_{off} \rangle}. \end{aligned} \tag{1.42}$$

We use the coefficient of variation squared to quantify noise in $\boldsymbol{x}$

$$CV_{\boldsymbol{x}}^2 \equiv \frac{\overline{\langle \boldsymbol{x}^2 \rangle} - \overline{\langle \boldsymbol{x} \rangle}^2}{\overline{\langle \boldsymbol{x} \rangle}^2} = \frac{\gamma(\langle e^{-\gamma \boldsymbol{\tau}_{off}} \rangle \langle e^{-\gamma \boldsymbol{\tau}_{on}} \rangle - 1) \langle \boldsymbol{\tau}_{off} \rangle \langle \boldsymbol{\tau}_{on} \rangle)}{(\langle e^{-\gamma \boldsymbol{\tau}_{off}} \rangle \langle e^{-\gamma \boldsymbol{\tau}_{on}} \rangle - 1) \gamma \langle \boldsymbol{\tau}_{on} \rangle^2} + \frac{(\langle \boldsymbol{\tau}_{on} \rangle + \langle \boldsymbol{\tau}_{off} \rangle)((\langle e^{-\gamma \boldsymbol{\tau}_{off}} \rangle - 1)(\langle e^{-\gamma \boldsymbol{\tau}_{on}} \rangle - 1)}{(\langle e^{-\gamma \boldsymbol{\tau}_{off}} \rangle \langle e^{-\gamma \boldsymbol{\tau}_{on}} \rangle - 1) \gamma \langle \boldsymbol{\tau}_{on} \rangle^2} + \frac{1}{2} \frac{1}{\overline{\langle \boldsymbol{x} \rangle}}. \tag{1.43}$$

The first two terms in the right-hand side of this equation show the contribution of random gene switching times in protein noise, the last term quantifies the contribution of random synthesis events. While the mean of protein is independent of statistical characteristic of switching times, the protein fluctuations depend on the entire distribution of $\boldsymbol{\tau}_{on}$ and $\boldsymbol{\tau}_{off}$.

Next, based on the measurements inside the living cells [6], we assume that gene deactivation reaction happens in exponentially distributed time intervals and we explore the effect of noise in gene activation time interval. Fig. 3 shows that making gene-activation reaction more noisy increases $CV_{\boldsymbol{x}}^2$. Further, we can approximate the results in the limit of fast gene switching as

$$CV_{\boldsymbol{x}}^2 \approx \frac{1}{2} \frac{\langle \boldsymbol{\tau}_{on} \rangle^2 \gamma}{\langle \boldsymbol{\tau}_{on} \rangle + \langle \boldsymbol{\tau}_{off} \rangle} \left(1 + CV_{\boldsymbol{\tau}_{on}}^2\right) + \frac{1}{2} \frac{1}{\overline{\langle \boldsymbol{x} \rangle}}, \tag{1.44}$$

where $CV_{\boldsymbol{\tau}_{on}}^2 \equiv \langle \boldsymbol{\tau}_{on}^2 \rangle / \langle \boldsymbol{\tau}_{on} \rangle^2 - 1$ denotes the coefficient of variation squared of gene-activation time intervals. This equation clearly shows that the noise in gene activation reaction increases the noise in protein concentration. Moreover, this equation quantifies the contribution of decay rate on noise, i.e., higher decay rate means higher noise. Additionally, this equation shows that noise in $\boldsymbol{x}$ depends on both fluctuations and amplitude of gene-switching time intervals (Fig. 3). Finally, in the limit of slow gene switching, noise in $\boldsymbol{x}$ is independent of noise in gene-switching time intervals

$$CV_{\boldsymbol{x}}^2 \approx \frac{\langle \boldsymbol{\tau}_{off} \rangle}{\langle \boldsymbol{\tau}_{on} \rangle} + \frac{1}{2} \frac{1}{\overline{\langle \boldsymbol{x} \rangle}}. \tag{1.45}$$

1.6 Conclusion

We studied statistical moments of a class of stochastic hybrid systems with multiple operation modes. We derived exact solution of the first and second order

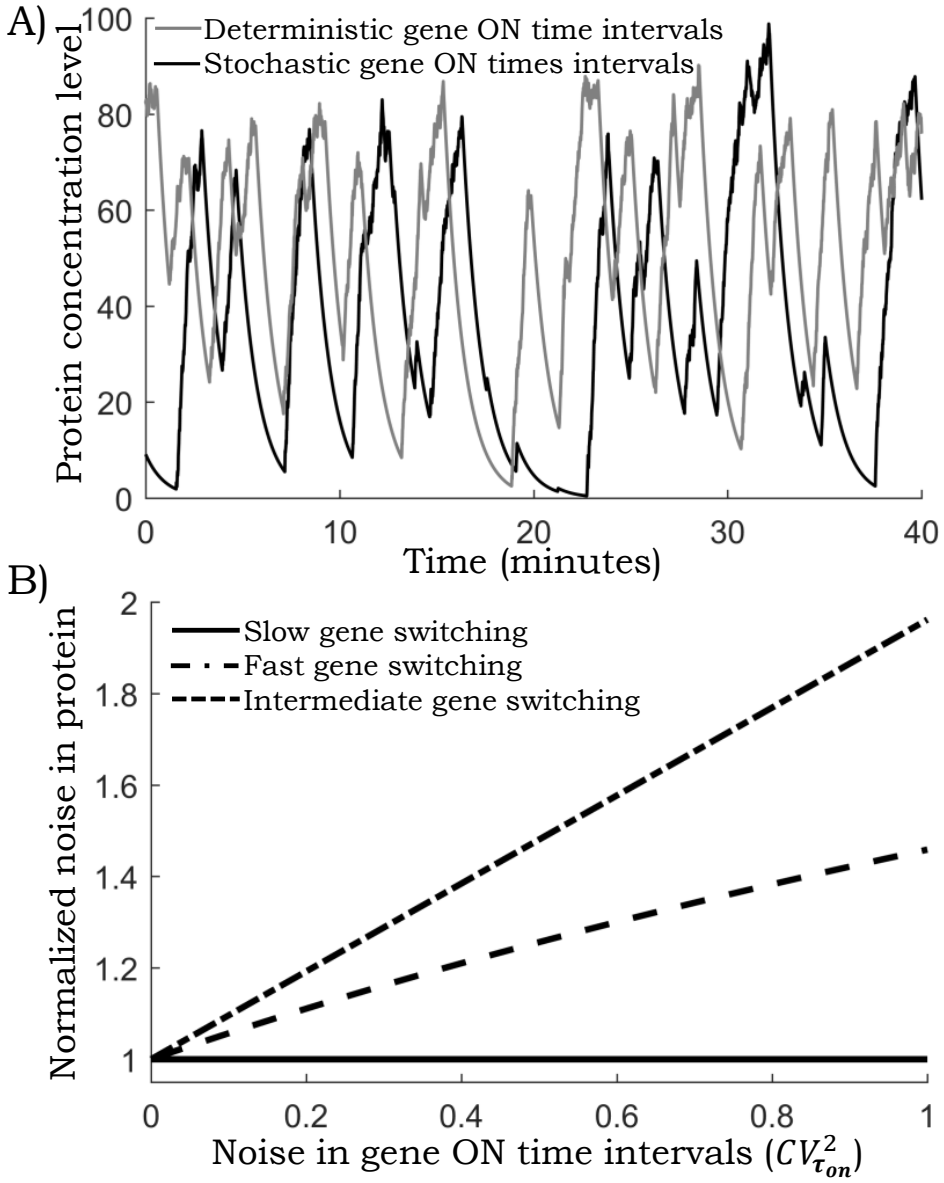

Figure 1.3. The noise in protein concentration is highly affected by the gene-switching time intervals. A) Noise in gene ON time intervals will not change the mean of a protein. Moreover, it does not have an obvious effect on the protein time trend. B) The noise in protein is highly affected by the gene switching noise. While the mean of protein only depends on the ratio of gene ON and OFF times, noise is affected by the magnitude of the ON and OFF time intervals as well. For this plot the protein production rate is selected to be $k = 100$, decay rate is $\gamma = 1\ min^{-1}$, and mean ON and OFF time intervals are equal $\langle \boldsymbol{\tau}_{on} \rangle = \langle \boldsymbol{\tau}_{off} \rangle$.

moments as well as necessary and sufficient conditions for having finite moments. While we only present our derivations for a two mode system, the results can be generalized

to a any arbitrary number of modes.

We used the framework presented here to calculate the mean and the noise in protein concentration. We find that the randomness in gene-activation time intervals increases the noise in protein while having no effect on the mean. Hence noise can be used to infer protein expression parameters systematically. Noise in gene-activation time intervals is an indicator of the number of steps that needs to be taken to activate a gene [6]. Previously through a numerical model we explored this connection on experimental data obtained from mouse [6]. Here we provide the exact solutions that can be used to infer mechanisms behind gene switching in different types of cells.

The continuous dynamics here are governed via a set of time-invariant SDEs. Our preliminary results show that some classes of time-varying differential equations have closed set of moments. Changing dynamics of the modes to time-varying differential equations will be the case of future efforts. Moreover, here we only allowed occurrence of one reset in each operation mode. Our previous work addressed multiple families of resets for a system with only one operational mode [55]. Future works will consider inclusion of multiple families of resets for each mode.

Chapter 2

TIME-TRIGGERED STOCHASTIC HYBRID SYSTEM WITH TWO TIMER DEPENDENT RESET

We analyze a class of time-triggered stochastic hybrid systems where the state-space evolves as per a linear time-invariant dynamical system. This continuous time evolution is interspersed with two kinds of stochastic resets. The first reset occurs based on an internal timer that measures the time elapsed since it last occurred. Whenever the first reset occurs the states-space undergoes a random jump and the timer is reset to zero. The second reset occurs based an arbitrary timer-depended rate, and whenever this reset fires, the state-space is changed based on a given random map. For this class of systems, we provide exact conditions that lead to finite statistic moments, and the corresponding exact analytical expressions for the first two moments. This framework is applied to study random fluctuations in the concentration of a protein in a growing cell. In the context of this example, the timer denotes the time elapsed since the cell was born, and the cell division event (first reset) is trigged based on a timer-dependent rate. The second reset corresponds to synthesis of the protein in stochastic bursts, and finally, during cell growth protein concentration continuously decrease due to dilution. Our analysis provides closed-form formulas for the noise in the protein concentration and leads to a striking result - noise in the concentration is invariant of the noise in the cell-cycle time. We also investigate how protein noise levels change for different forms of production rate that depend on the internal timer, as is the case for cell-cycle regulated genes inside the cell.

2.1 Model Formulation

The state space of the SHS $\boldsymbol{x} \in \mathbb{R}^{n\times 1}$ evolves as per a linear time-invariant system

$$\dot{\boldsymbol{x}}(t) = \hat{a} + A\boldsymbol{x}, \tag{2.1}$$

with a constant matrix $A \in \mathbb{R}^{n\times n}$ and vector $\hat{a} \in \mathbb{R}^{n\times 1}$. This continuous time evolution of the state space is interspersed by two families of random resets, which we describe in further detail below.

2.1.1 First family of resets

The first family of resets is assumed to occurs at times $\boldsymbol{t}_s$, $s \in \{1, 2, 3, \ldots\}$, such that the time intervals $\boldsymbol{\tau}_s \equiv \boldsymbol{t}_s - \boldsymbol{t}_{s-1}$ are independent and identically distributed random variable following an arbitrary positively-valued continuous probability density function (pdf) f. To model the timing of these resets we introduce a timer $\boldsymbol{\tau}$ that linearly increases over time

$$\dot{\boldsymbol{\tau}} = 1, \tag{2.2}$$

and resets to zero

$$\boldsymbol{\tau} \mapsto 0 \tag{2.3}$$

whenever the event occurs. The occurrence of the next event depends on state of the timer introducing memory in the event-arrival process. More specifically, the probability that an event occurs in the next infinitesimal time interval $(t, t + dt]$ is given by $h_1(\boldsymbol{\tau})dt$, where the *hazard rate*

$$h_1(\tau) \equiv \frac{f(\tau)}{1 - \int_{y=0}^{\tau} f(y)dy}. \tag{2.4}$$

Defining the arrival of events as per (2.10) ensures that $\boldsymbol{\tau}_s$ follows the pdf f

$$\boldsymbol{\tau}_s \sim f(\tau) = h_1(\tau)e^{-\int_{y=0}^{\tau} h_1(y)dy}, \tag{2.5}$$

and the corresponding pdf of $\boldsymbol{\tau}$ is given by (see Appendix A)

$$\boldsymbol{\tau} \sim p(\tau) = \frac{1}{\langle \boldsymbol{\tau}_s \rangle} e^{-\int_{y=0}^{\tau} h_1(y)dy}. \tag{2.6}$$

For example, if f is exponentially-distributed with mean $\langle \boldsymbol{\tau}_s \rangle$, then $h_1(\tau) = 1/\langle \boldsymbol{\tau}_s \rangle$ would be a constant corresponding to a Poisson arrival of events.

Having modeled the timing of the first family of resets, we next describe its impact on the SHS state space. Each time the event occurs, the state of system undergoes a random jump as per the reset

$$\boldsymbol{x} \mapsto \boldsymbol{x}_{1^+}, \boldsymbol{\tau} \mapsto 0, \tag{2.7}$$

where $\boldsymbol{x}_1^+$ is the state of a system immediately after an event belonging to the first family of resets. We assume $\boldsymbol{x}_{1^+}$ to be a random variable whose statistics depends on the value of $\boldsymbol{x}$ just before the event.

iand its statisics a random variable of which mean is a linear affine map of states' value before the first reset

$$\langle \boldsymbol{x}_{1^+} \rangle = J_1 \boldsymbol{x} + \hat{r}_1, \tag{2.8}$$

where $J_1 \in \mathbb{R}^{n \times n}$ and $\hat{r}_1 \in \mathbb{R}^{n \times 1}$ are a constant matrix and vector, respectively. Further, we define a state dependent noise form

$$\begin{aligned} &\langle \boldsymbol{x}_{1^+} \boldsymbol{x}_{1^+}^\top \rangle - \langle \boldsymbol{x}_{1^+} \rangle \langle \boldsymbol{x}_{1^+}^\top \rangle = \\ &Q_1 \boldsymbol{x} \boldsymbol{x}^\top Q_1^\top + B_1 \boldsymbol{x} \hat{c}_1^\top + \hat{c}_1 \boldsymbol{x} B_1^\top + G_1, \end{aligned} \tag{2.9}$$

where $Q_1 \in \mathbb{R}^{n \times n}$, $B_1 \in \mathbb{R}^{n \times n}$ are constant matrices. $G_1 \in \mathbb{R}^{n \times n}$ is a constant symmetric positive semi-definite matrix, and $\hat{c}_1 \in \mathbb{R}^{n \times 1}$ is a constant vector. Based on (2.14), the covariance matrix of $\boldsymbol{x}_{1^+}$ depends on $\boldsymbol{x}$ where noise term match the quadratic and linear function of system state. [54]

Having defined this timer, one can now define a corresponding *hazard rate*

$$h_1(\tau) \equiv \frac{f(\tau)}{1 - \int_{y=0}^{\tau} f(y) dy}, \tag{2.10}$$

In our time-triggered stochastic hybrid model, we formulated two random resets (Fig.1.1); however, our model can easily extend to more random resets.

In addition, we introduce a measuring the time since the last first reset and resets to zero whenever the next first random event occurs

$$\boldsymbol{\tau} \mapsto 0. \tag{2.11}$$

Thereby, a timer-dependent hazard rate can be defined to ensure that time interval $\boldsymbol{\tau}_s$ between two successive first random event following a given arbitrary probability distribution function; thus, probability of the first random event happeningwhere y and τ are dummy variables. Thus, the time interval $\boldsymbol{\tau}_s$ follows a probability density function f

2.1.1.1 The first random reset

We assume the first random reset occurring in the next infinitesimal interval $(t, t+dt]$ with probability $h_1(\boldsymbol{\tau})dt$. After a random event occurring, the state of system resets as

$$\boldsymbol{x} \mapsto \boldsymbol{x}_{1^+}, \boldsymbol{\tau} \mapsto 0, \tag{2.12}$$

where $\boldsymbol{x}_{1^+}$, denoting states of a system after the first reset, is a random variable of which mean is a linear affine map of states' value before the first reset

$$\langle \boldsymbol{x}_{1^+} \rangle = J_1 \boldsymbol{x} + \hat{r}_1, \tag{2.13}$$

where $J_1 \in \mathbb{R}^{n\times n}$ and $\hat{r}_1 \in \mathbb{R}^{n\times 1}$ are constant matrix and vector, respectively. Further, we define a state dependent noise form

$$\begin{aligned} &\langle \boldsymbol{x}_{1^+} \boldsymbol{x}_{1^+}^\top \rangle - \langle \boldsymbol{x}_{1^+} \rangle \langle \boldsymbol{x}_{1^+}^\top \rangle = \\ &Q_1 \boldsymbol{x}\boldsymbol{x}^\top Q_1^\top + B_1 \boldsymbol{x} \hat{c}_1^\top + \hat{c}_1 \boldsymbol{x} B_1^\top + G_1, \end{aligned} \tag{2.14}$$

where $Q_1 \in \mathbb{R}^{n\times n}$, $B_1 \in \mathbb{R}^{n\times n}$ are constant matrices. $G_1 \in \mathbb{R}^{n\times n}$ is a constant symmetric positive semi-definite matrix, and $\hat{c}_1 \in \mathbb{R}^{n\times 1}$ is a constant vector. Based on (2.14), the covariance matrix of $\boldsymbol{x}_{1^+}$ depends on $\boldsymbol{x}$ where noise term match the quadratic and linear function of system state. [54]

2.1.1.2 The second random reset

Similarly, the probability of second random reset will happen in the next infinitesimal time $(t, t+dt]$ is $h_2(\boldsymbol{\tau})dt$. The reset map for the second random reset is

$$\boldsymbol{x} \mapsto \boldsymbol{x}_{2^+}, \tag{2.15}$$

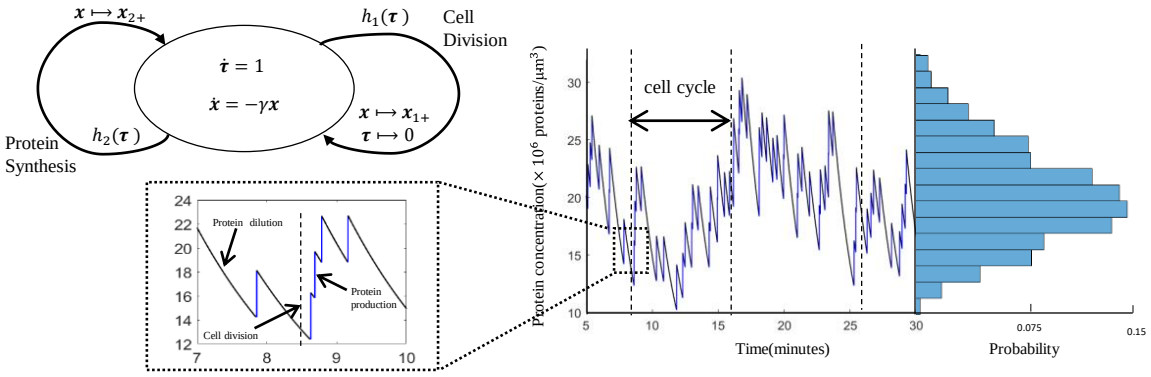

Figure 2.1. Modeling protein concentration in a single cell using time-triggered stochastic hybrid system *Right*: Protein level $x \in R$ is modeled by SHS with two generally distributed stochastic resets, which are protein synthesis event and cell division event, in a single cell. Cell division time interval is tracked by timer $\boldsymbol{\tau}$; whenever Cell division occurs, the state reset follow (2.16) and timer resets to 0. Additionally, the steady state distribution of protein concentration is simulated by a large number Monte Carlo method. *Left top*: Sketch of mathematical model for protein concentration. Protein concentration is diluted at rate γ. Protein burst size is a random variable $\boldsymbol{u}$. Cell division dose not affect mean of protein concentration. *Left bottom*: zoom-in figure for part of protein concentration evolving with time.

where $\boldsymbol{x}_{2^+}$ denotes states of a system after the second random reset. Same as the first random reset in (2.13), we have (2.16) relation between mean of states of a system after second random reset and states of a system before second random reset

$$\langle \boldsymbol{x}_{2^+} \rangle = J_2 \boldsymbol{x} + \hat{r}_2, \tag{2.16}$$

where $J_2 \in \mathbb{R}^{n \times n}$ and $\hat{r}_2 \in \mathbb{R}^{n \times 1}$ are constant matrix and vector, respectively. Furthermore, the second family random event rest covariance matrix is same as (2.14) by replacing Q_2,B_2,$\hat{c}_2$,G_2 with their respective.

2.1.2 Biology Example

Our model is motivated by stochastic fluctuations in gene expression occurring during transcription and translation process [5,11,29,61], triggering variation at protein concentration in a single cell [1,4,12,14,31,38,40,54,56,57]. We will briefly describe this biology phenomenon to connect with mathematical model to further interpret model.

we assume that protein degradation is a deterministic process, and protein concentration is diluted at a constant rate γ. By that means, we can write continuous dynamics of protein as

$$\dot{\boldsymbol{x}}(t) = -\gamma \boldsymbol{x}, \tag{2.17}$$

comparing with (2.1), we could find parameters in our model for continuous dynamics of protein concentration as $A = -\gamma$, $\hat{a} = 0$. Instead of a matrix , A is a scalar in the biology example; same as $\hat{a}$.

The first random reset is cell divisions, happening at end of cell-cycle time interval. Cell divisions will cause protein copy number and cell size variation randomly; thus, cell division is one of essential reasons causing protein fluctuation in a single cell [10,16,26,49]. $\boldsymbol{\tau}_s$ is time intervals between cell division, defined as a cell cycle time. Additionally, mean of cell-cycle time ($\langle \boldsymbol{\tau}_s \rangle$) has the following relation with dilution rate [2]

$$\langle \boldsymbol{\tau}_s \rangle = \frac{\ln 2}{2\gamma}, \tag{2.18}$$

In our biology example, we assume symmetric division in a single cell. Accordingly, when cell division event occurs, protein copy numbers and cell volume reduce by half; thus, average protein concentration has no change. Especially, states of the system are same before and after first random reset; based on (2.13), the first random reset can be written as

$$\langle \boldsymbol{x}_{1^+} \rangle = \boldsymbol{x}. \tag{2.19}$$

When cell division happens, each protein molecule follow binomial distribution to be separated into one of two daughter cells. Such random binomial division introduce noise in protein concentration, represented as

$$\langle \boldsymbol{x}_{1^+}^2 \rangle - \langle \boldsymbol{x}_{1^+} \rangle^2 = b\boldsymbol{x}, \tag{2.20}$$

where $b \in \mathbb{R}^+$ quantify the dispersion of protein division. Comparing with (2.13) and (2.14), we can have reset parameters for the first family random event as $J_1 = 1$, $B_1 = b/2$, $\hat{c}_1 = 1$ and $\hat{r}_1 = Q_2 = G_1 = 0$.

The second random reset is protein synthesis event. During cell-cycle time, protein synthesis rate vary on different cell-cycle phase [23], and stochasticity of gene expression cause fluctuation in protein synthesis [24]. Thus, we assume each synthesis event increases the protein count by a identical and independent distributed random variable $\boldsymbol{u}$. Random variable $\boldsymbol{u}$ has mean $\langle \boldsymbol{u} \rangle$ and variance$\langle \boldsymbol{u}^2 \rangle - \langle \boldsymbol{u} \rangle^2$. Thus, the second random reset express as

$$\langle \boldsymbol{x}_{2^+} \rangle = \boldsymbol{x} + \langle \boldsymbol{u} \rangle. \tag{2.21}$$

According (2.13) and (2.16), we can identify random event reset parameters for the second random reset as $J_2 = 1$, and $\hat{r}_2 = \langle \boldsymbol{u} \rangle$. The noise only comes from protein synthesis size, thus $Q_2 = R_2 = \hat{c}_2 = 0$ and $G_2 = \langle \boldsymbol{u}^2 \rangle$.

Motivated by randomness of protein synthesis process and cell-cycle division process, we formulated a mathematical model to describe the system. In Fig.2.1, we give the sketch of our biologic system and one trajectory simulation of the system with both stochastic protein synthesis and cell division events. Since our mathematical model is well defined, we will investigate statistical properties of the system in the next section.

2.2 Statistical Moments

As all components of the system have been defined in 2.1, we will present our novel method to find statistic moments for time-triggered stochastic hybrid system, instead of using Monte Carlo simulation.

2.2.1 The first-order moment

The conditional mean of time-variant system evolves as

$$\frac{\partial \langle \boldsymbol{x} | \boldsymbol{\tau} \rangle}{\partial t} = \hat{a}_x(y) + A_x(y) \langle \boldsymbol{x} | \boldsymbol{\tau} \rangle \tag{2.22}$$

where

$$\begin{aligned} A_x(y) &= A + h_2(y)(J_2 - I_n), \\ \hat{a}_x(y) &= \hat{a} + \hat{r}_2 h_2(y), \end{aligned} \tag{2.23}$$

Here, one can see that the conditional mean of systems change to time variant system, and conditional mean of time-variant system can derived as

$$\begin{aligned}\langle \boldsymbol{x}|\boldsymbol{\tau}=\tau\rangle &= e^{\int_0^{\boldsymbol{\tau}} A_x(y)dy}\,\langle \boldsymbol{x}|\boldsymbol{\tau}=0\rangle \\ &\quad + e^{\int_0^{\boldsymbol{\tau}} A_x(y)dy}\int_0^{\tau} e^{-\int_0^{l} A_x(y)dy}\hat{a}(l)dl\end{aligned} \tag{2.24}$$

where $\langle \boldsymbol{x}|\boldsymbol{\tau}=0\rangle$ is the first order moment of the system before the first family reset. In order to calculate $\overline{\langle \boldsymbol{x}|\boldsymbol{\tau}=0\rangle}$, We apply (2.13)

$$\overline{\langle \boldsymbol{x}|\boldsymbol{\tau}=0\rangle} = J_1\overline{\langle \boldsymbol{x}|\boldsymbol{\tau}=\boldsymbol{\tau}_s\rangle} \tag{2.25}$$

As $\boldsymbol{\tau}\mapsto 0$, we have $\boldsymbol{x}|\boldsymbol{\tau}=\tau\mapsto \boldsymbol{x}|\boldsymbol{\tau}=0$. Thus, $\overline{\langle \boldsymbol{x}|\boldsymbol{\tau}=0\rangle}$ can solve as

$$\begin{aligned}\overline{\langle \boldsymbol{x}|\boldsymbol{\tau}=0\rangle} &= (I_n - J_1\langle e^{\int_0^{\boldsymbol{\tau}_s} A_x(y)dy}\rangle)^{-1}\hat{r}_1 \\ &\quad + J_1\langle e^{\int_0^{\boldsymbol{\tau}_s} A_x(y)dy}\int_0^{\boldsymbol{\tau}_s} e^{-\int_0^{l} A_x(y)dy}\hat{a}(l)dl\rangle\end{aligned} \tag{2.26}$$

Finally, we use (2.6) to uncondition (2.26) with respect to $\boldsymbol{\tau}$ to get the result in Theorem 1.

Theorem 3 *Consider two random resets time-triggered stochastic hybrid system, linear continuous dynamics is given as (2.1), and two random resets satisfy (2.2)-(2.16). If and only if all eigenvalues of* $J_1\left\langle e^{\int_0^{\boldsymbol{\tau}_s} A_x(y)dy}\right\rangle$ *are inside the unit circle, the first-order moment can be finite and solved as*

$$\begin{aligned}\overline{\langle \boldsymbol{x}\rangle} &= \left\langle e^{\int_0^{\boldsymbol{\tau}} A_x(y)dy}\right\rangle (I_n - J_1\left\langle e^{\int_0^{\boldsymbol{\tau}_s} A_x(y)dy}\right\rangle)^{-1}\times \\ &\left(\left\langle J_1 e^{\int_0^{\boldsymbol{\tau}_s} A_x(y)dy}\int_0^{\boldsymbol{\tau}_s} e^{-\int_0^{l} A_x(y)dy\boldsymbol{\tau}}\hat{a}_x(l)dl\right\rangle + \hat{r}_1\right) \\ &+ \left\langle e^{\int_0^{\boldsymbol{\tau}} A_x(y)dy}\int_0^{\boldsymbol{\tau}} e^{-\int_0^{l} A_x(y)dy}\hat{a}_x(l)dl\right\rangle,\end{aligned} \tag{2.27}$$

where

$$\begin{aligned}A_x(y) &= A + h_2(y)(J_2 - I_n), \\ \hat{a}_x(y) &= \hat{a} + \hat{r}_2 h_2(y),\end{aligned} \tag{2.28}$$

■

Corollary 1 *Assume a system described as (2.1)-(2.16) with $h_2(\boldsymbol{\tau}) = 0$, system is simplified to only one timer depended resets. First order moment of the system is*

$$\begin{aligned}\overline{\langle \boldsymbol{x} \rangle} = \left\langle e^{A\boldsymbol{\tau}} \right\rangle (I_n - J_1 \left\langle e^{A\boldsymbol{\tau}_s} \right\rangle)^{-1} \times \left(\left\langle J_1 e^{A\boldsymbol{\tau}_s} \int_0^{\boldsymbol{\tau}_s} e^{-Al} \hat{a} dl \right\rangle \right. \\ \left. + \hat{r}_1 \right) + \left\langle e^{A\boldsymbol{\tau}} \int_0^{\boldsymbol{\tau}} e^{-Al} \hat{a} dl \right\rangle .\end{aligned} \tag{2.29}$$

Corollary 2 *Assume a system described as (2.1)-(2.16) with $A = 0$, $h_2(\boldsymbol{\tau}) = 0$; and all eigenvalues of the matrix J_1 are inside the unit circle, first-order moment of the system is*

$$\overline{\langle \boldsymbol{x} \rangle} = (I_n - J_1)^{-1}(J_1 \langle \boldsymbol{\tau}_s \rangle + \hat{r}_1) + \frac{\langle \boldsymbol{\tau}_s^2 \rangle}{2\langle \boldsymbol{\tau}_s \rangle} \hat{a}, \tag{2.30}$$

depending only on the first and second order moment of $\boldsymbol{\tau}_s$.

2.2.2 The second-order moments

In order to calculate the second-order moments of system, we introduce vectorization transformation which linearly transfer a matrix into a column vector. The second-order dynamics $\boldsymbol{x}\boldsymbol{x}^\top$ follows

$$\frac{d(\boldsymbol{x}\boldsymbol{x}^\top)}{dt} = A\boldsymbol{x}\boldsymbol{x}^\top + \boldsymbol{x}\boldsymbol{x}^\top A^\top + \hat{a}\boldsymbol{x}^\top + \boldsymbol{x}\hat{a}^\top, \tag{2.31}$$

By using Vectorization transformation, (2.31) can rewrite as

$$\begin{aligned}\frac{d\text{vec}\left(\boldsymbol{x}\boldsymbol{x}^\top\right)}{dt} &= (I_n \otimes A + A \otimes I_n) \text{vec}\left(\boldsymbol{x}\boldsymbol{x}^\top\right) \\ &\quad + (I_n \otimes \hat{a} + \hat{a} \otimes I_n)\boldsymbol{x},\end{aligned} \tag{2.32}$$

where $\text{vec}(\boldsymbol{x}\boldsymbol{x}^\top) \in \mathbb{R}^{n^2 \times 1}$ denotes as vector representation of matrix $\boldsymbol{x}\boldsymbol{x}^\top \in \mathbb{R}^{n \times n}$. $\otimes$ stands the Kronecker Product.

In order to obtain as similar form of second order moment as (2.1), we define a new vector

$$\boldsymbol{\mu} \equiv [\boldsymbol{x}^\top \ \text{vec}(\boldsymbol{x}\boldsymbol{x}^\top)^\top]^\top, \tag{2.33}$$

thus, based on (2.1) and (2.32), the dynamics of $\boldsymbol{\mu}$ follows

$$\dot{\boldsymbol{\mu}} = \hat{a}_\mu + A_\mu \boldsymbol{\mu}, \tag{2.34}$$

where

$$A_\mu = \left[\begin{array}{c|c} A & 0 \\ \hline I_n \otimes \hat{a} + \hat{a} \otimes I_n & I_n \otimes A + A \otimes I_n \end{array}\right], \\ \hat{a}_\mu = \left[\begin{array}{c} \hat{a} \\ \hline 0 \end{array}\right]. \tag{2.35}$$

When the first family and second family reset occurs, the states of $\boldsymbol{\mu}$ reset as

$$\boldsymbol{\mu}_{i^+} = J_{\mu_i}\boldsymbol{\mu} + \hat{r}_{\mu_1}, i \in \{1, 2\}, \tag{2.36}$$

where

$$J_{\mu_i} \equiv \left[\begin{array}{c|c} J_i & 0 \\ \hline B_i \otimes \hat{c}_i + \hat{c}_i \otimes B_i & \\ +J_i \otimes \hat{r}_i + \hat{r}_i \otimes J_i & J_i \otimes J_i + Q_i \otimes Q_i \end{array}\right], \tag{2.37}$$

$$\hat{r}_{\mu_i} \equiv \left[\begin{array}{c} \hat{r}_i \\ \hline \mathrm{vec}(G_i + \hat{r}_i\hat{r}_i^\top) \end{array}\right]. \tag{2.38}$$

We can observe that continuous time dynamics (2.34) is similar to (2.1), and stochastic resets (2.36) are similar to (2.13). With a similar approach analyzing in Theorem 1, we can find finite second order moments of $\boldsymbol{x}$.

Theorem 4 *The system follows* (2.1)-(2.14) *and satisfies Theorem 1.* $\boldsymbol{x}\boldsymbol{x}^\top$ *can solve through the vector* $\boldsymbol{\mu}$*. The steady state of* $\boldsymbol{\mu}$ *exist if and only if all the eigenvalues of the matrix* $(J_1 \otimes J_1 + Q_1 \otimes Q_1)\left\langle e^{\int_0^{\boldsymbol{\tau}_s} A_{\mu'}(y)dy} \otimes e^{\int_0^{\boldsymbol{\tau}_s} A_{\mu'}(y)dy}\right\rangle$ *are inside the unit circle.*

$$\begin{aligned} \overline{\langle\boldsymbol{\mu}\rangle} &= \left\langle e^{\int_0^{\boldsymbol{\tau}} A_{\mu'}(y)dy}\right\rangle (I_n - J_{\mu_1}\left\langle e^{\int_0^{\boldsymbol{\tau}_s} A_{\mu'}(y)dy}\right\rangle)^{-1} \times \\ &\left(\left\langle J_{\mu_1} e^{\int_0^{\boldsymbol{\tau}_s} A_{\mu'}(y)dy} \int_0^{\boldsymbol{\tau}_s} e^{-\int_0^l A_{\mu'}(y)dy}\hat{a}_{\mu'}(l)dl\right\rangle + \hat{r}_{\mu_1}\right) \\ &+ \left\langle e^{\int_0^{\boldsymbol{\tau}} A_{\mu'}(y)dy} \int_0^{\boldsymbol{\tau}} e^{-\int_l^{\boldsymbol{\tau}} A_{\mu'}(y)dy}\hat{a}_{\mu'}(l)dl\right\rangle, \end{aligned} \tag{2.39}$$

where

$$\begin{aligned} A_{\mu'}(y) &= A_\mu + h_2(y)(J_{\mu_2} - I_{n^2+n}), \\ \hat{a}_{\mu'}(y) &= \hat{a}_\mu + \hat{r}_{\mu_2}h_2(y). \end{aligned} \tag{2.40}$$

■

In this section, we give theorems to solve the first and second order moment; however, it can easily extend to solve high order moment by same approaches. We will give an example in the next section to apply these theorems.

2.3 Biology Example

We have briefly introduced a biology example with connection to the mathematical model in 2.1.2, and we also gave theorems in 2.2 to solve first- and second-order moments of our mathematical model. Therefore, we will apply theorems into the biology example to explore moments of the system.

Here, we quickly review defined parameters in protein concentration. The system has continuous dynamics as $A = -\gamma$, $\hat{a} = 0$. For cell division events, the system has $J_1 = 1$, $B_1 = b/2$, $\hat{c}_1 = 1$, $\hat{r}_1 = Q_1 = G_1 = 0$. For protein synthesis events, system are taken $J_2 = 1$, $\hat{r}_2 = \langle \boldsymbol{u} \rangle$, $Q_2 = R_2 = \hat{c}_2 = 0$, $G_2 = \langle \boldsymbol{u}^2 \rangle$.

In order to quantify Fano factor of protein concentration, we need to solve the mean and the variance of protein concentration. Given the Theorem 1 & 2, we first define a new vector $\boldsymbol{\mu} \equiv [\boldsymbol{x} \quad \boldsymbol{x}^2]^\top$. According (2.35), the dynamics of $\boldsymbol{\mu}$ be written as

$$A_\mu = \begin{bmatrix} -\gamma & 0 \\ 0 & -2\gamma \end{bmatrix}, \hat{a}_\mu = \begin{bmatrix} 0 \\ 0 \end{bmatrix}. \tag{2.41}$$

After stochastic protein synthesis event, based on (2.37) and (2.38), reset map of the states can be written as

$$J_{\mu_2} = \begin{bmatrix} 1 & 0 \\ 2\langle \boldsymbol{u} \rangle & 1 \end{bmatrix}, \hat{r}_{\mu_2} = \begin{bmatrix} \langle \boldsymbol{u} \rangle \\ \langle \boldsymbol{u}^2 \rangle \end{bmatrix}, \tag{2.42}$$

Applying (2.40), the matrices $A_{\mu'}(y)$ and $\hat{a}_{\mu'}(y)$ are shown as

$$\begin{aligned} A_{\mu'}(y) &= \begin{bmatrix} -\gamma & 0 \\ 2h_2(y)\langle \boldsymbol{u} \rangle & -2\gamma \end{bmatrix}, \\ \hat{a}_{\mu'}(y) &= \begin{bmatrix} h_2(y)\langle \boldsymbol{u} \rangle \\ h_2(y)\langle \boldsymbol{u}^2 \rangle \end{bmatrix}. \end{aligned} \tag{2.43}$$

After a cell division, protein concentration level reset in (2.36) as

$$J_{\mu_1} = \begin{bmatrix} 1 & 0 \\ b & 1 \end{bmatrix}, \hat{r}_{\mu_1} = \begin{bmatrix} 0 \\ 0 \end{bmatrix}. \tag{2.44}$$

Given the above setup matrices, we can use (2.39) to derive the first order moment of protein concentration as

$$\begin{aligned} \overline{\langle \boldsymbol{x} \rangle} = & \frac{\langle \boldsymbol{u} \rangle}{\gamma \langle \boldsymbol{\tau}_s \rangle} \langle e^{-\gamma \boldsymbol{\tau}_s} \int_0^{\boldsymbol{\tau}_s} e^{\gamma l} h_2(l) dl \rangle \\ & + \langle \boldsymbol{u} \rangle \langle e^{-\gamma \boldsymbol{\tau}} \int_0^{\boldsymbol{\tau}} e^{\gamma l} h_2(l) dl \rangle, \end{aligned} \tag{2.45}$$

and the second order moment of protein concentration is shown on (2.31).

$$\begin{aligned} \overline{\langle \boldsymbol{x}^2 \rangle} = & \frac{\langle e^{-\gamma \boldsymbol{\tau}_s} \int_0^{\boldsymbol{\tau}_s} e^{\gamma l} h_2(l) dl \rangle}{2\gamma^2 \langle \boldsymbol{\tau}_s \rangle (1 - \langle e^{-\gamma \boldsymbol{\tau}_s} \rangle)} (-b\gamma \langle e^{-\gamma \boldsymbol{\tau}_s} \rangle + 2\langle \boldsymbol{u} \rangle (\langle \frac{\int_0^{\boldsymbol{\tau}_s} h_2(l) dl e^{-\gamma \boldsymbol{\tau}_s}}{\boldsymbol{\tau}_s} \rangle \\ & - \langle \frac{\int_0^{\boldsymbol{\tau}_s} h_2(l) dl e^{-2\gamma \boldsymbol{\tau}_s}}{\boldsymbol{\tau}_s} \rangle)) + 2\gamma \langle \boldsymbol{\tau}_s \rangle (\langle \frac{\int_0^{\boldsymbol{\tau}} h_2(l) dl e^{-2\gamma \boldsymbol{\tau}}}{\boldsymbol{\tau}} \rangle - \langle \frac{\int_0^{\boldsymbol{\tau}} h_2(l) dl \tau e^{-\gamma \boldsymbol{\tau}}}{\boldsymbol{\tau}} \rangle) \\ & + \frac{\langle e^{\int_0^{\boldsymbol{\tau}_s} (-\gamma + h_2(l)) dl} \int_0^{\boldsymbol{\tau}_s} e^{-\int_0^{\boldsymbol{\tau}} (-\gamma + h_2(l)) dl} \langle \boldsymbol{u}^2 \rangle h_2(l) dl \rangle}{2\gamma \langle \boldsymbol{\tau}_s \rangle} \\ & + \langle e^{\int_0^{\boldsymbol{\tau}} (-\gamma + h_2(l)) dl} \int_0^{\boldsymbol{\tau}} e^{-\int_0^{\boldsymbol{\tau}} (-\gamma + h_2(l)) dl} \langle \boldsymbol{u}^2 \rangle h_2(l) dl \rangle. \end{aligned} \tag{2.31}$$

2.3.1 Constant protein synthesis rate

In the first place, we consider a simplest case which is a constant protein synthesis rate

$$h_2(\boldsymbol{\tau}) = k, \tag{2.32}$$

substituting into (2.45) and (2.31), we can solve the mean and Fano factor (FF) of protein concentration after applying (2.18)

$$\overline{\langle \boldsymbol{x} \rangle} = \frac{k \langle \boldsymbol{u} \rangle}{\gamma}, \tag{2.33}$$

$$FF = \frac{\overline{\langle \boldsymbol{x}^2 \rangle} - \overline{\langle \boldsymbol{x} \rangle}^2}{\overline{\langle \boldsymbol{x} \rangle}^2} = \frac{\langle \boldsymbol{u}^2 \rangle}{2\langle \boldsymbol{u} \rangle} + \frac{b}{\ln 2}. \tag{2.34}$$

One can observe that there are two terms in the Fano factor (FF) of protein concentration: (2.34) shows that variation of FF comes from protein synthesis and cell division. Furthermore, cell-cycle times dose not affect FF of protein concentration in a cell; in other words, FF of protein concentration is independent of statistical characteristics of cell-cycle times when protein synthesis rate is constant.

2.3.2 Time varying protein synthesis rate

Next, we will explore time varying protein synthesis rate. First, assuming protein synthesis rate is a linearly increasing function of timer,

$$h_2(\tau) = k\tau, \tag{2.35}$$

applying (2.45) to solve mean of protein as

$$\overline{\langle \boldsymbol{x} \rangle} = \frac{k\langle \boldsymbol{u} \rangle \langle \boldsymbol{\tau} \rangle}{\gamma} = \frac{k\langle \boldsymbol{u} \rangle \ln 2}{\gamma^2}(CV^2_{\boldsymbol{\tau}_s} + 1), \tag{2.36}$$

where $CV^2_{\boldsymbol{\tau}_s}$ is noise (squared coefficient of variation) of cell division. One can observe that mean of protein is dependent on the noise of cell division, and high noise of cell division system will have large mean value; in other words, if a system has a constant mean of protein concentration, large mean of protein synthesis value have low noise.

Additionally, if we assume the protein synthesis rate is a special decreasing function of timer

$$h_2(\tau) = \tau e^{-k\tau}, \tag{2.37}$$

Mean of protein concentration is

$$\overline{\langle \boldsymbol{x} \rangle} = \frac{2\langle \boldsymbol{u} \rangle}{k \ln 2}(1 - e^{\frac{-k \ln 2}{2\gamma}}) \tag{2.38}$$

We plot the mean of protein concentration in Fig.3 representing constant protein synthesis rate and both increasing and decreasing protein synthesis rate. One can observe that as constant k increasing, mean of protein concentration increase both at constant protein synthesis rate and increasing protein synthesis rate, which is reasonable. However, for the decreasing protein synthesis, mean of protein concentration decrease as k increasing.

Further, we plot the fano factor of protein concentration under different protein synthesis rates to investigate how cell-cycle time affect fano factor of protein concentration. As we discussed before, when protein synthesis rate is constant, fano factor of protein concentration will not be affected by the cell-cycle time. Also, we could observe fano factor of protein concentration present U-shape when protein synthesis rates is linear increasing function of cell-cycle time. However, fano factor of protein concentration is monotonically decreasing if protein synthesis rate is under decreasing function $\tau e^{-k\tau}$.

2.4 Conclusion

In this paper, we formulate a mathematical model to explore statistical properties of protein concentration. We form a specific types of stochastic hybrid system which is piece-wise time-triggered stochastic hybrid system with two random resets where moment of the system can be solved directly without any approximation. The first random reset of the system, coming from cell-division, occurs based on an arbitrary distributed timer (cell-cycle time). the second random reset of the system is protein synthesis of which probability is dependent on cell-cycle time. We find a novel method to derive the exact first- and second- order moment of the system, and apply our derived moments to the protein concentration inside a single cell. We discussed the behavior of Fano factor of the protein concentration inside a single cell with different protein synthesis rate. If proteins has a constant synthesis rate, mean and Fano factor of protein concentration are independent on statistical properties of cell-cycle time. However, if protein synthesis rate is a linearly increasing function with respect to cell-cycle time, with fixed constant mean level protein concentration in side a single cell, longer cell-cycle time has lower noise of protein concentration. Moreover, for other special protein synthesis rates, mean and Fano factor of protein concentration are dependent on the cell-cycle time distribution. Finally, we plot the Fano factor of protein concentration with respect to a deterministic cell-cycle time. Interestingly, any constant protein synthesis rate has Also, we find that exponentially increasing protein

synthesis rate achieve lower noise in protein concentration comparing with linearly increasing protein synthesis rate.

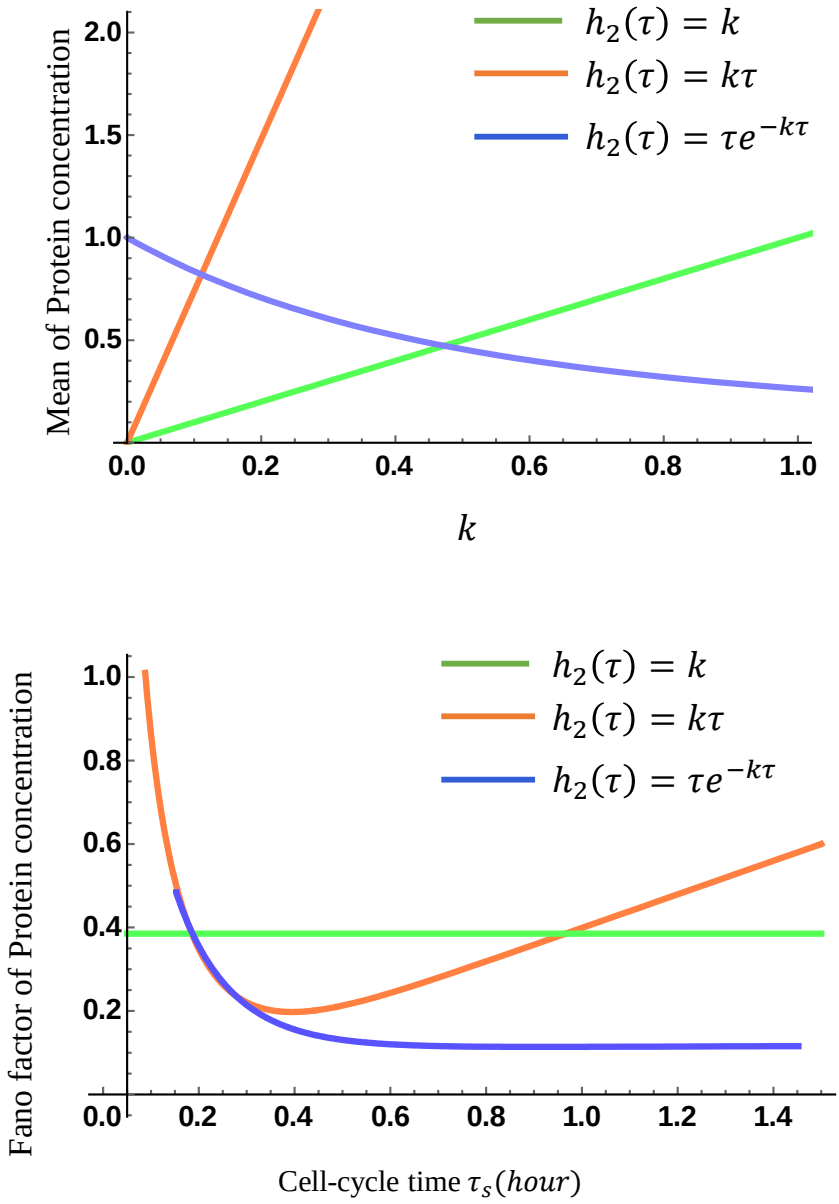

Figure 2.2. Deterministic Cell-cycle time affect Fano factor of protein concentration with different protein synthesis rate. When protein synthesis is a constant, Fano Factor of protein concentration has a monotonically decreasing function with respect to cell-cycle time. The other two protein synthesis rates cause a non-monotonically decreasing function of Fano Factor of protein synthesis. In both cases, an optimal cell-cycle time can be determined to have a minimal Fano Factor value of protein concentration. Fano Factor for protein synthesis $\tau e^{k\tau}$ increase much sharply at long cell-cycle time. Parameters are taken value as: $\langle \boldsymbol{u}^2 \rangle = 2$, $\langle \boldsymbol{u} \rangle = 1\mu g/ml$, $k = 1h^{-1}$, $\gamma = 5\mu g/ml \cdot h^{-1}$, $b = 1$.

Chapter 3

NOISE ANALYSIS IN BIOCHEMICAL COMPLEX FORMATION

Several biological functions are carried out via complexes that are formed via multimerization of either a single species (homomers) or multiple species (heteromers). Given functional relevance of these complexes, it is presumably desired to maintain their level at a set point and minimize fluctuations around it. Here we consider two simple models of complex formation – one for homomer and another for heteromer of two species – and analyze effect of important model parameters on the noise in complex level. In particular, we study the effect of (i) sensitivity of the complex formation rate with respect to constituting species' abundance, and (ii) relative stability of the complex as compared with that of the constituents. By employing an approximate moment analysis, we find that for a given steady state level, there is an optimal sensitivity that minimizes noise (quantified by fano-factor; variance/mean) in the complex level. Furthermore, the noise becomes smaller if the complex is less stable than its constituents. Finally, for the heteromer case, our findings show that noise is enhanced if the complex is comparatively more sensitive to one constituent. We briefly discuss implications of our result for general complex formation processes.

3.1 Stochastic Model Formulation

In this section, we describe two simple models of complex formation (Fig. 3.1). The first model consists of a single species that forms a homomer, whereas the second model consists of two species that combine to form a heteromer.

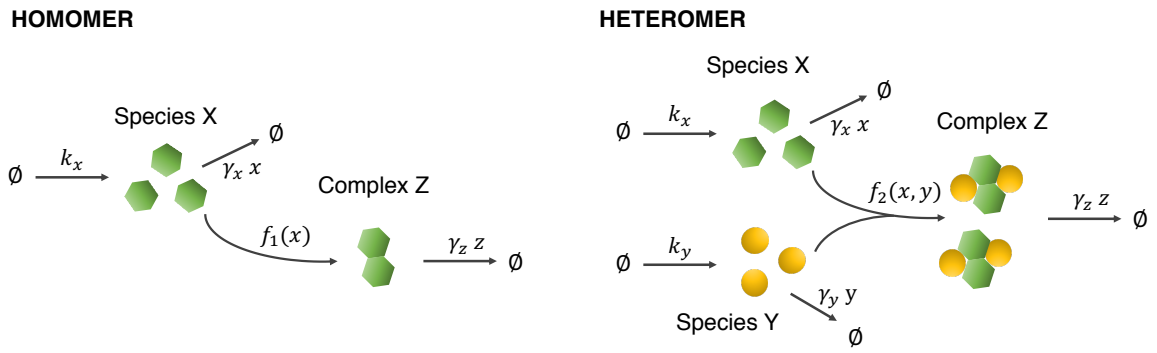

Figure 3.1. Schematic for complex formation. *Top:* A species X is produced at a rate k_x and its n_x molecules combine to form a complex (homomer), Z, with rate $f_1(x)$. The species X and the complex Z degrade enzymatically with rates $\gamma_x x$ and $\gamma_z z$ respectively. *Bottom:* Two species, X and Y, are respectively produced at rates k_x and k_y. n_x molecules of X combine with n_y molecules of Y to form a complex (heteromer), Z, with rate $f_2(x, y)$. Both constituting species and the complex decay enzymatically with corresponding rates $\gamma_x x$, $\gamma_y y$ and $\gamma_z z$.

3.1.1 Homomer

Consider the following biochemical system that comprises of production and degradation of a species, X. Furthermore, n_x molecules of X interact to form a complex Z, which can also degrade.

$$\emptyset \xrightarrow{k_x} X, \qquad X \xrightarrow{\gamma_x x} \emptyset, \tag{3.1a}$$

$$n_x X \xrightarrow{f_1(x)} Z, \qquad Z \xrightarrow{\gamma_z z} \emptyset. \tag{3.1b}$$

Here the levels of species X and the complex Z are denoted by small letters x and z respectively. The production rates of X follows a zero-order kinetics with rate constant k_x while the complex Z is made with a rate $f_1(x)$ where f_1 denotes an arbitrary positive function in its argument. Assuming a mass action kinetics, $f_1(x)$ would take the form $k_1 x^{n_x}$ where $k_1 > 0$; however, other forms of $f_1(x)$ are also possible, e.g., Michelis-Menten, Hill Function, etc. While we do not assume a particular form of f_1, we assume that it satisfies the following properties:

(a) $\lim_{x\to 0^+} f_1(x) = 0$

(b) $f_1(x)$ is a monotonically increasing function in x.

These assumptions are made to ensure that the system in (3.1) has unique positive steady state. Finally, degradation of both X, and Z is assumed to follow first-order reaction kinetics with rates γ_x, and γ_z.

One way to describe the dynamics of the biochemical system in (3.1) is to use the ordinary differential equation (ODE) based approach. In this case, the following ODEs can be used to compute (x, z)

$$\frac{dx}{dt} = k_x - \gamma_x x - n_x f_1(x), \tag{3.2a}$$

$$\frac{dz}{dt} = -\gamma_z z + f_1(x). \tag{3.2b}$$

With the aforementioned assumptions on $f_1(x)$, it can be shown that $(x, z) \in \mathbb{R}^2_+$ is positively invariant for the dynamical system in (3.2). That is, if the system starts from an initial condition in $\mathbb{R}^2_+$, then it remains in that set. In addition, (3.2) has a unique steady-state in $(x_{ss}, z_{ss}) \in \mathbb{R}^2_+$ which is given by the real-valued solution to the following algebraic system

$$0 = k_x - \gamma_x x_{ss} - n_x f_1(x_{ss}), \tag{3.3a}$$

$$0 = -\gamma_z z_{ss} + f_1(x_{ss}). \tag{3.3b}$$

We refer interested readers to Appendix A for a sketch of proof of these statements.

3.1.2 Heteromer

Next consider the scenario where two species X and Y interact to form the complex Z. The biochemical system now consists of production of X and Y, interaction between them to form Z, and degradation of all three of them

$$\emptyset \xrightarrow{k_x} X, \qquad X \xrightarrow{\gamma_x x} \emptyset, \tag{3.4a}$$

$$\emptyset \xrightarrow{k_y} Y, \qquad Y \xrightarrow{\gamma_y y} \emptyset, \tag{3.4b}$$

$$n_x X + n_y Y \xrightarrow{f_2(x,y)} Z, \qquad Z \xrightarrow{\gamma_z z} \emptyset. \tag{3.4c}$$

Here, the notations x and z have same meaning as the homomer case, and likewise y denotes the level of Y. The production rates of X and Y are k_x and k_y while the complex Z is made with a rate $f_2(x, y)$ where f_2 denotes an arbitrary positive function of its arguments. As in the homomer case, we do not assume a particular form of f_2. However in order to ensure that the system in (3.4) has unique positive steady state, we assume that it satisfies the following properties

(a) $\lim_{x\to 0^+} f_2(x, y) = 0$,

(b) $\lim_{y\to 0^+} f_2(x, y) = 0$,

(c) $f_2(x, y)$ is a monotonically increasing function in both its arguments.

Lastly, each of the species X, Y and Z are assumed to degrade enzymatically with rates γ_x, γ_y and γ_z respectively.

In a deterministic description, the time evolution of (x, y, z) is governed by the following system of differential equations

$$\frac{dx}{dt} = k_x - \gamma_x x - n_x f_2(x, y), \tag{3.5a}$$

$$\frac{dy}{dt} = k_y - \gamma_y y - n_y f_2(x, y), \tag{3.5b}$$

$$\frac{dz}{dt} = -\gamma_z z + f_2(x, y). \tag{3.5c}$$

With the previously mentioned assumptions on $f_2(x, y)$, it can be seen that (3.5) has a unique steady-state in $(x_{ss}, y_{ss}, z_{ss}) \in \mathbb{R}^3_+$ which is given by the real-valued solution to the algebraic system

$$0 = k_x - \gamma_x x_{ss} - n_x f_2(x_{ss}, y_{ss}), \tag{3.6a}$$

$$0 = k_y - \gamma_y y_{ss} - n_y f_2(x_{ss}, y_{ss}), \tag{3.6b}$$

$$0 = -\gamma_z z_{ss} + f_2(x_{ss}, y_{ss}). \tag{3.6c}$$

Sketch of the proof for these properties is provided in Appendix A.

While the above deterministic descriptions of homomer/heteromer can provide insights into some important system behaviors (e.g., response times), they fail in accounting for stochastic effects. The stochasticity naturally arises from the probabilistic nature of reactions, but it becomes particularly prominent when the reacting species are present in low copy numbers [45] . Our focus in this work is to analyze the stochastic behavior of the system, particularly the noise in complex level. To this end, we provide stochastic descriptions of the systems in (3.1) and (3.4) in the subsequent section.

3.2 Stochastic Models and Moment Equations

Let $\mathbf{x}(t)$, $\mathbf{y}(t)$ and $\mathbf{z}(t)$ respectively denote the molecular counts of X, Y and Z (the species Y is only applicable for the heteromer case). While $\mathbf{x}(t)$, $\mathbf{y}(t)$, $\mathbf{z}(t)$ are stochastic processes, we will omit the explicit dependence on time unless the context demands it. The time evolution of these can be described via probabilities of various events happening in an infinitesimal time-interval $(t, t+dt]$. We describe the detailed stochastic models for both cases in Table 3.1.

Ideally one needs to solve the chemical master equation in order to fully characterize a stochastic model [17, 59]. However, here we are only interested in studying the noise in complex level. Therefore, we directly use the dynamical equations to compute first two moments. Below we provide moment equations for both homomer and heteromer models of the complex formation process.

3.2.1 Moment Dynamics for Homomer

Using standard tools from stochastic systems [17, 59], the time evolution of expected value of a monomial $\mathbf{x}^{m_1}\mathbf{z}^{m_2}$, with $m_1, m_2 \in \mathbb{N}$, can be written as

$$\begin{aligned}\frac{d\mathbb{E}[\mathbf{x}^{m_1}\mathbf{z}^{m_2}]}{dt} = \mathbb{E}[k_x\left((\mathbf{x}+1)^{m_1}\mathbf{z}^{m_2} - \mathbf{x}^{m_1}\mathbf{z}^{m_2}\right) + f_1(\mathbf{x})\left((\mathbf{x}-n_x)^{m_1}(\mathbf{z}+1)^{m_2} - \mathbf{x}^{m_1}\mathbf{z}^{m_2}\right) \\ + \gamma_x\mathbf{x}\left((\mathbf{x}-1)^{m_1}\mathbf{z}^{m_2} - \mathbf{x}^{m_1}\mathbf{z}^{m_2}\right) + \gamma_z\mathbf{z}\left(\mathbf{x}^{m_1}(\mathbf{z}-1)^{m_2} - \mathbf{x}^{m_1}\mathbf{z}^{m_2}\right)]. \quad (3.7)\end{aligned}$$

Here order of a moment is given by the sum $m_1 + m_2$.

An important point to note is that if the complex formation rate, $f_1(\mathbf{x})$, is constant or a linear affine function of $\mathbf{x}$, then dynamics of a moment of a certain order can be described in terms of moments of same or lower order. However, if $f_1(\mathbf{x})$ is is nonlinear, then moment dynamics is not closed: dynamics of a moment depends on moments of order higher than it. This is referred to as the problem of moment closure. Several *moment closure* methods that provide approximation to moment dynamics have been proposed in literature [8, 18, 19, 21, 28, 34, 37, 44–46, 48, 50, 58]. These methods are based on several themes such as linearization, neglecting some higher order moments/cumulants, assumptions on underlying distribution, preservation of some

Table 3.1. Description of Stochastic Models for Complex Formation

Model	Event	Population Reset Function	Propensity
5*__Homomer__	Production of X	$\mathbf{x}(t) \mapsto \mathbf{x}(t) + 1$	k_x
	Degradation of X	$\mathbf{x}(t) \mapsto \mathbf{x}(t) - 1$	$\gamma_x \mathbf{x}(t)$
	Production of Z	$\mathbf{z}(t) \mapsto \mathbf{z}(t) + 1$	$f_1(\mathbf{x})$
		$\mathbf{x}(t) \mapsto \mathbf{x}(t) - n_x$	$f_1(\mathbf{x})$
	Degradation of Z	$\mathbf{z}(t) \mapsto \mathbf{z}(t) - 1$	$\gamma_z \mathbf{z}(t)$
8*__Heteromer__	Production of X	$\mathbf{x}(t) \mapsto \mathbf{x}(t) + 1$	k_x
	Degradation of X	$\mathbf{x}(t) \mapsto \mathbf{x}(t) - 1$	$\gamma_x \mathbf{x}(t)$
	Production of Y	$\mathbf{y}(t) \mapsto \mathbf{y}(t) + 1$	k_y
	Degradation of Y	$\mathbf{y}(t) \mapsto \mathbf{y}(t) - 1$	$\gamma_y \mathbf{y}(t)$
	Production of Z	$\mathbf{z}(t) \mapsto \mathbf{z}(t) + 1$	$f_2(\mathbf{x}, \mathbf{y})$
		$\mathbf{x}(t) \mapsto \mathbf{x}(t) - n_x$	$f_2(\mathbf{x}, \mathbf{y})$
		$\mathbf{y}(t) \mapsto \mathbf{y}(t) - n_y$	$f_2(\mathbf{x}, \mathbf{y})$
	Degradation of Z	$\mathbf{z}(t) \mapsto \mathbf{z}(t) - 1$	$\gamma_z \mathbf{z}(t)$

dynamical, physical or moment properties , etc. [28, 48]. In this paper, we use a linearization technique called linear noise approximation wherein the nonlinear propensity $f_1(\mathbf{x})$ is linearized around the deterministic solution to (3.1) [44, 59]. This technique is known to give accurate approximations in the limit of low noise.

Recall that because of our assumptions on the function $f_1(x)$, the system (3.1) has a unique, positive, real equilibrium point. Assuming small fluctuations in $(\mathbf{x}, \mathbf{z})$ around the steady-state deterministic solution (x_{ss}, z_{ss}), we linearize $f_1(\mathbf{x})$ and substitute the linearized form in (3.7). More specifically, we take

$$f_1(\mathbf{x}) = f_1(x_{ss}) \left(1 + S_x \frac{\mathbf{x} - x_{ss}}{x_{ss}}\right), \tag{3.8a}$$

where

$$S_x = \frac{\partial \log f_1(\mathbf{x})}{\partial \log \mathbf{x}} |_{x_{ss}}, \tag{3.8b}$$

is the log sensitivity of $f_1(\mathbf{x})$ with respect to $\mathbf{x}$. Plugging (3.8) in (3.7), the dynamics of first two moments of each of the species can be obtained. We then use these to compute approximate first two stationary moments of the complex Z and eventually compute the noise in Z.

3.2.2 Moment Dynamics for Heteromer

Next we consider the heterodimer wherein X and Y combine to form the complex Z. In this case, expected value of a monomial $\mathbf{x}^{m_1}\mathbf{y}^{m_2}\mathbf{z}^{m_3}$, with $m_1, m_2, m_3 \in \mathbb{N}$, is governed by the following ODE

$$\begin{aligned}\frac{d\mathbb{E}[\mathbf{x}^{m_1}\mathbf{y}^{m_2}\mathbf{z}^{m_3}]}{dt} = \mathbb{E}[&k_x\left((\mathbf{x}+1)^{m_1}\mathbf{y}^{m_2}\mathbf{z}^{m_3} - \mathbf{x}^{m_1}\mathbf{y}^{m_2}\mathbf{z}^{m_3}\right) + k_y\left(\mathbf{x}^{m_1}(\mathbf{y}+1)^{m_2}\mathbf{z}^{m_3}\right.\\ &\left. - \mathbf{x}^{m_1}\mathbf{y}^{m_2}\mathbf{z}^{m_3}\right) + f_2(\mathbf{x},\mathbf{y})\left((\mathbf{x}-n_x)^{m_1}(\mathbf{y}-n_y)^{m_2}(\mathbf{z}+1)^{m_3} - \mathbf{x}^{m_1}\mathbf{y}^{m_2}\mathbf{z}^{m_3}\right)\\ &+ \gamma_x\mathbf{x}\left((\mathbf{x}-1)^{m_1}\mathbf{y}^{m_2}\mathbf{z}^{m_3} - \mathbf{x}^{m_1}\mathbf{y}^{m_2}\mathbf{z}^{m_3}\right) + \gamma_y\mathbf{y}\left(\mathbf{x}^{m_1}(\mathbf{y}-1)^{m_2}\mathbf{z}^{m_3} - \mathbf{x}^{m_1}\mathbf{y}^{m_2}\mathbf{z}^{m_3}\right)\\ &+ \gamma_z\mathbf{z}\left(\mathbf{x}^{m_1}\mathbf{y}^{m_2}(\mathbf{z}-1)^{m_3} - \mathbf{x}^{m_1}\mathbf{y}^{m_2}\mathbf{z}^{m_3}\right)]. \quad (3.9)\end{aligned}$$

As with the homomer case, the assumptions on $f_2(\mathbf{x},\mathbf{y})$ imply that (3.4) has a unique, positive, real equilibrium point. We can linearize $f_2(\mathbf{x},\mathbf{y})$ around the steady-state deterministic solution (x_{ss}, y_{ss}, z_{ss}) More specifically, we take

$$f_2(\mathbf{x},\mathbf{y}) = f_2\left(x_{ss}, y_{ss}\right)\left(1 + S_x\frac{\mathbf{x}-x_{ss}}{x_{ss}} + S_y\frac{\mathbf{y}-y_{ss}}{y_{ss}}\right), \quad (3.10a)$$

where

$$S_x = \frac{\partial \log f_2(\mathbf{x},\mathbf{y})}{\partial \log \mathbf{x}}\Big|_{(x_{ss},y_{ss})}, \quad S_y = \frac{\partial \log f_2(\mathbf{x},\mathbf{y})}{\partial \log \mathbf{y}}\Big|_{(x_{ss},y_{ss})}, \quad (3.10b)$$

are the log sensitivities of $f(\mathbf{x},\mathbf{y})$ with respect to $\mathbf{x}$ and $\mathbf{y}$. Plugging (3.10) in (3.9), the dynamics of first two moments of each of the species can be obtained. We can use symbolic computations in Mathematica for this purpose. It turns out that the form of the second moment of Z is quite convoluted, which subsequently results in convoluted expression for the fano factor FF_Z. We do not provide those expressions here and only provide formula for FF_Z for a simple case wherein $S_x = S_y$, $x_{ss} = y_{ss}$, $\gamma_x = \gamma_y$, and $n_x = n_y$ (see the next Section). For other cases, we have to rely on numerical computation.

3.3 Analysis of Noise Properties of the Complex

In this section, we analyze how various parameters in the complex formation process affect the noise in the complex level. For this purpose, we quantify the noise in

Z using fano factor (variance/mean). We investigate the effect of varying the sensitivity with respect to one of the constituents and relative degradation rate of the complex as compared with those of its constituents.

3.3.1 Steady-State Noise in Homomer level

To systematically analyze the effect of important model parameters on the noise, we keep the steady-state means in the linearized model constant (note that they are exactly same as the deterministic steady-state solution to (3.1)). More specifically, we find the production rate of X in terms of other model parameters and fixed steady-state means (x_{ss}, z_{ss})

$$k_x = \gamma_x x_{ss} + n_x \gamma_z z_{ss}, \tag{3.11}$$

Using this we obtain the following expression for the fano factor (FF_Z)

$$FF_Z = -\frac{S_x z_{ss}(2r x_{ss}(n_x - S_x) + n_x S_x z_{ss}(n_x - 1))}{2(r x_{ss} + n_x S_x z_{ss})(((r+1)x_{ss} + n_x S_x z_{ss}))} + 1, \tag{3.12}$$

where $r = \gamma_x/\gamma_z$ is the ratio of degradation rates of the species X and the complex Z.

Analyzing the above formula provides several important insights in to how noise is affected by various parameters. For example, FF_Z varies non-monotonically with respect to sensitivity S_x. When the sensitivity is small, production rate of Z is approximately constant. Indeed FF_Z takes a value close to one, which corresponds to a Poisson limit (Fig. 3.2, Top). With increase in S_x, the noise first decreases and increases back after an optimal value. Further, if the number of molecules required to form the homomer, i.e., n_x, is increased then the overall noise profile shifts downwards, which suggests that a homomer made of more molecules is better in terms of noise suppression.

It is also important to point out that we have treated S_x and n_x separately since we consider a general form of $f_1(x)$. However, if $f_1(x)$ is assumed to follow a mass-action kinetics, then it can be easily checked from (3.8) that $S_x = n_x$. For this

reason, we only consider the values of S_x between 0 to n_x to be physiologically relevant and accordingly scale the S_x axis in Fig. 3.2.

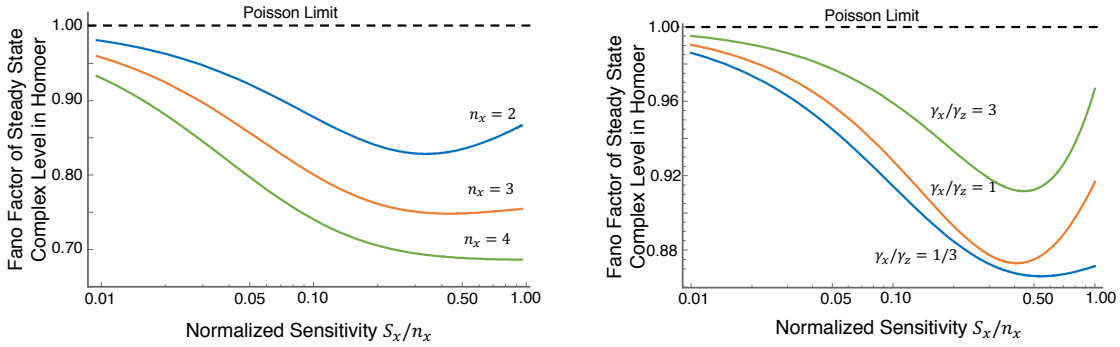

Figure 3.2. Noise in complex level as a function of sensitivity of complex formation rate with respect to the species, and relative degradation rates of the complex and the species. *Top*: The noise in complex level shows a non-monotonic behavior with increase in the sensitivity (normalized by the stoichiometry). The noise further decreases when the stoichiometry of the species in the complex formation process is is higher, suggesting that a higher order multimer can suppress noise better. The noise approaches the Poisson limit of low sensitivity values. *Bottom:*. The non-monotonic curve between noise and sensitivity shifts upwards as the relative degradation rates of the species and the complex are increased. Thus, the noise increases when the complex is relatively unstable than the species.

In addition to S_x, we also investigate how stability of the species X and the complex Z determine the noise in Z. To this end, we note that the fano factor in (3.12) only depends on the parameter $r = \gamma_x/\gamma_z$, and not on individual values of the degradation rates. Also, we can find the limit of FF_Z for large/small r as

$$\lim_{r\to 0} FF_Z = 1 - \frac{S_x z_{ss}(n_x - 1)}{2(x_{ss} + n_x S_x z_{ss})}, \qquad \lim_{r\to\infty} FF_Z = 1. \tag{3.13}$$

As shown in Fig. 3.2 (Bottom), increasing γ_x/γ_z shifts the noise vs sensitivity curve upwards.Thus, making the complex relatively unstable with respect to the species results in lower noise in the complex.

3.3.2 Steady-State Noise in Heteromer level

As in the homomer case above, we analyze the noise in the heteromer level while maintaining the steady-state of the system at some (x_{ss}, y_{ss}, z_{ss}). To this end,

the production rates of X and Y are varied such that the following hold

$$k_x = \gamma_x x_{ss} + n_x \gamma_z z_{ss}, \tag{3.14a}$$

$$k_y = \gamma_y y_{ss} + n_y \gamma_z z_{ss}. \tag{3.14b}$$

It turns out that while the expression for the fano factor FF_Z is quite complicated for a general case, a simpler form can be obtained for a special case when $n_x = n_y$, $S_x = S_y$ and $\gamma_x = \gamma_y$.

$$FF_Z = \frac{S_x z_{ss}(2r(S_x - n_x)x_{ss} + (1 - 2n_x)n_x S_x z_{ss})}{(rx_{ss} + 2n_x S_x z_{ss})((r+1)x_{ss} + 2n_x S_x z_{ss})} + 1. \tag{3.15}$$

Note that in this case x_{ss} is equal to y_{ss}, while $r = \gamma_x/\gamma_z$. A close examination of (3.15) shows that it resembles (3.12) except for some scaling factors. Not surprisingly, even in this case varying S_x produces a non-monotonic, U-shape behavior for noise in Z (we do not show the results here). We further look at how the results change when $S_x \neq S_y$. Interestingly, it is seen that the noise always increases in this case, showing that if the complex formation rate is more sensitive to one constituent than another then its results in a higher noise in the complex level (Fig. 3.3).

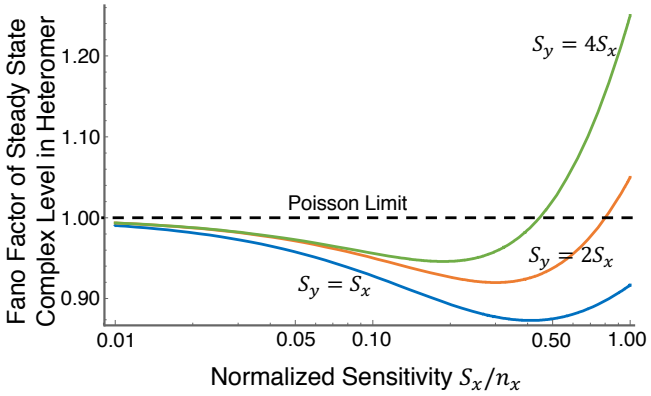

Figure 3.3. Noise in complex level when complex formation rate has different sensitivities to each constituent. While the noise behavior shows non-monotonic profile with increase in sensitivity with respect to a constituent, the curve shifts upwards as the sensitivities of both species are changed. This implies that a symmetric sensitivity is better for noise suppression.

3.4 Conclusion and Future Work

In this paper, we analyzed two simple models of biochemical complex formation. The first model was of a homomer that is formed from a single species, whereas the second model was of a heteromer of two species. We explored the effect of two parameters in the models: (i) sensitivity of the complex formation rate to the species, and (ii) relative stability of the species and the complex. Key insights from our analysis are:

- For a homomer, its steady state noise shows a non-monotonic behavior as the sensitivity of the complex formation rate to the species level is changed. Moreover, the noise in complex level reduces when the complex is relatively unstable as compared to the species.
- For a heteromer, the noise exhibits similar behavior as in the homomer case if sensitivities and other parameters of both species are exactly same. However, when the complex formation rate is more sensitive to one species, then noise in the complex increases.

While these results are derived for simple cases, the similarity between noise behaviors of complexes made of one and two species suggests that they may hold even for complexes consisting of additional species. Since many complexes that occur in biochemical systems are made of multiple species [63], studying their noise behavior and relating it to their function would be an important direction of future research. It would also be interesting to explore reversible kinetics for the complex formation (i.e., Z dissociates to its constituents), and also self-regulation in production of the species as found in production of a range of proteins [15, 30, 36].

BIBLIOGRAPHY

[1] Jochen Kumm Aaron E Hirsh, Guri Giaever and Michael B Eisen. Noise minimization in eukaryotic gene expression. *PLOS Biology*, 2:e137, 2004.

[2] Uri Alon. *An introduction to systems biology: design principles of biological circuits*. Chapman and Hall/CRC, 2006.

[3] Ariel Amir. Cell size regulation in bacteria. *Physical Review Letters*, 112:208102, 2014.

[4] Narendra Maheshri Miri Carmi Erin O'Shea Yitzhak Pilpel Arren Bar-Even, Johan Paulsson and Naama Barkai. Noise in protein expression scales with natural protein abundance. *Nature Genetics*, 38:636–643, 2006.

[5] Nathalie Q Balaban and Jack Merrin. Bacterial persistence as a phenotypic switch. *Science*, 305:1622–1625, 2004.

[6] Linda R. Petzold Bernie J. Daigle, Mohammad Soltani and Abhyudai Singh. Inferring single-cell gene expression mechanisms using stochastic simulation. *Bioinformatics*, 31:1428–1435, 2015.

[7] Brooke Trinh Brian Munsky and Mustaf Khammash. Listening to the noise: random fluctuations reveal gene network parameters. *Molecular Systems Biology*, 5:318, 2009.

[8] Kyeong-Hun Kim Chang Hyeong Lee and Pilwon Kim. A moment closure method for stochastic reaction networks. *Journal of Chemical Physics*, 130:134107, 2009.

[9] David Gatfield1 Kim Schneider1 Ueli Schibler David M. Suter, Nacho Molina and Felix Naef. Mammalian genes are transcribed with widely different bursting kinetics. *Science*, 332:472–474, 2011.

[10] Stefano Di Talia, Jan M Skotheim, James M Bean, Eric D Siggia, and Frederick R Cross. The effects of molecular noise and size control on variability in the budding yeast cell cycle. *Nature*, 448(7156):947, 2007.

[11] Avigdor Eldar and Michael B Elowitz. Functional roles for noise in genetic circuits. *Nature*, 467:167–173, 2010.

[12] Theodore J. Perkins Eric Libby and Peter S. Swain. Noisy information processing through transcriptional regulation. *Proceedings of the National Academy of Sciences*, 104:7151–7156, 2007.

[13] Maxim Finkelstein. Failure rate and mean remaining lifetime. In *Failure Rate Modelling for Reliability and Risk*, Springer Series in Reliability Engineering, pages 9–44. Springer, 2008.

[14] Bärbel Finkenstädt, Dan J Woodcock, Michal Komorowski, Claire V Harper, Julian RE Davis, Mike RH White, David A Rand, et al. Quantifying intrinsic and extrinsic noise in gene transcription using the linear noise approximation: An application to single cell data. *The Annals of Applied Statistics*, 7(4):1960–1982, 2013.

[15] Paul François and Vincent Hakim. Core genetic module: the mixed feedback loop. *Physical Review E*, 72:031908, 2005.

[16] Nir Friedman, Long Cai, and X Sunney Xie. Linking stochastic dynamics to population distribution: an analytical framework of gene expression. *Physical review letters*, 97(16):168302, 2006.

[17] Crispin Gardiner. *Stochastic Methods*, volume 4. Springer Berlin, 2009.

[18] Khem Raj Ghusinga, Andrew G. Lamperski, and Abhyudai Singh. Moment analysis of stochastic hybrid systems using semidefinite programming. 2018.

[19] Khem Raj Ghusinga, Cesar A Vargas-Garcia, Andrew Lamperski, and Abhyudai Singh. Exact lower and upper bounds on stationary moments in stochastic biochemical systems. *Physical Biology*, 14:04LT01, 2017.

[20] Khem Raj Ghusinga, Cesar A. Vargas-Garcia, and Abhyudai Singh. A mechanistic stochastic framework for regulating bacterial cell division. *Scientific Reports*, page 30229, 2016.

[21] Colin S Gillespie. Moment-closure approximations for mass-action models. *IET Systems Biology*, 3:52–58, 2009.

[22] Daniel T. Gillespie. The chemical Langevin equation. *Journal of Chemical Physics*, 113:297–306, 2000.

[23] A Fukuda H Iba and Y Okada. Rate of major protein synthesis during the cell cycle of caulobacter crescentus. *Journal of bacteriology*, 135(2):647–655, 1978.

[24] Dann Huh and Johan Paulsson. Random partitioning of molecules at cell division. *Proceedings of the National Academy of Sciences*, 108(36):15004–15009, 2011.

[25] Scott M. Zawilski Ido Golding, Johan Paulsson and Edward C. Cox. Real-time kinetics of gene activity in individual bacteria. *Cell*, 123:1025–1036, 2005.

[26] A. L. Koch and M. Schaechter. A model for statistics of the cell division process. *Journal of General Microbiology*, 29:435–454, 1962.

[27] Bernt ksendal. *Stochastic differential equations*. Springer, 2003.

[28] Christian Kuehn. Moment closure brief review. In *Control of Self-Organizing Nonlinear Systems*, pages 253–271. Springer, 2016.

[29] Edo Kussell and Stanislas Leibler. Phenotypic diversity, population growth, and information in fluctuating environments. *Science*, 309:2075–2078, 2005.

[30] Bruno Lannoo, Enrico Carlon, and Marc Lefranc. Heterodimer autorepression loop: a robust and flexible pulse-generating genetic module. *Physical Review Letters*, 117:018102, 2016.

[31] Ben Lehner. Selection to minimise noise in living systems and its implications for the evolution of gene expression. *Molecular Systems Biology*, 4:170, 2008.

[32] Hugo Daniel Macedo and Jose Nuno Oliveira. Typing linear algebra: A biproduct-oriented approach. *Science of Computer Programming*, 78:2160–2191, 2013.

[33] Angeliki Magklara and Stavros Lomvardas. Stochastic gene expression in mammals: lessons from olfaction. *Trends in Cell Biology*, 23:449–456, 2014.

[34] James H Matis and Thomas R Kiffe. On interacting bee/mite populations: a stochastic model with analysis using cumulant truncation. *Environmental and Ecological Statistics*, 9:237–258, 2002.

[35] Nicholas Hastings Merran Evans and Brian Peacock. *Statistical Distributions*. Wiley, 3rd edition, 2000.

[36] Ron Milo, Shai Shen-Orr, Shalev Itzkovitz, Nadav Kashtan, Dmitri Chklovskii, and Uri Alon. Network motifs: simple building blocks of complex networks. *Science*, 298:824–827, 2002.

[37] Ingemar Nåsell. An extension of the moment closure method. *Theoretical Population Biology*, 64:233–239, 2003.

[38] Gregor Neuert, Brian Munsky, Rui Zhen Tan, Leonid Teytelman, Mustafa Khammash, and Alexander van Oudenaarden. Systematic identification of signal-activated stochastic gene regulation. *Science*, 339:584–587, 2013.

[39] Arjun Raj and Alexander van Oudenaarden. Nature, nurture, or chance: stochastic gene expression and its consequences. *Cell*, 135:216–226, 2008.

[40] Jonathan M. Raser and Erin K. O'Shea. Noise in gene expression: Origins, consequences, and control. *Science*, 309:2010 – 2013, 2005.

[41] Sheldon M. Ross. Reliability theory. In *Introduction to Probability Models*, pages 579–629. Academic Press, tenth edition, 2010.

[42] Abhyudai Singh Thomas V. Trimeloni James M. McCollum Chris D. Cox Michael L. Simpson Roy D. Dar, Brandon S. Razooky and Leor S. Weinberger. Transcriptional burst frequency and burst size are equally modulated across the human genome. *Proceedings of the National Academy of Sciences*, 109:17454–17459, 2012.

[43] Abhyudai Singh. Transient changes in intercellular protein variability identify sources of noise in gene expression. *Biophysical Journal*, 107:2214–2220, 2014.

[44] Abhyudai Singh and Ramon Grima. The linear-noise approximation and moment-closure approximations for stochastic chemical kinetics. *ArXiv Preprint ArXiv:1711.07383*, 2017.

[45] Abhyudai Singh and João P Hespanha. Stochastic hybrid systems for studying biochemical processes. *Philosophical Transactions of the Royal Society of London A: Mathematical, Physical and Engineering Sciences*, 368:4995–5011, 2010.

[46] Abhyudai Singh and João P Hespanha. Approximate moment dynamics for chemically reacting systems. *IEEE Transactions on Automatic Control*, 56:414–418, 2011.

[47] Lok-Hang So, Anandamohan Ghosh, Chenghang Zong, Leonardo A Sepúlveda, Ronen Segev, and Ido Golding. General properties of transcriptional time series in escherichia coli. *Nature Genetics*, 43:554–560, 2011.

[48] Leslaw Socha. *Linearization methods for stochastic dynamic systems*, volume 730. Springer Science & Business Media, 2007.

[49] Mahommad Soltani, Cesar A. Vargas-Garcia, Duarte Antunes, and Abhyudai Singh. Intercellular variability in protein levels from stochastic expression and noisy cell cycle processes. *PLOS Computational Biology*, page e1004972, 2016.

[50] Mahommad Soltani, Cesar A. Vargas-Garcia, and Abhyudai Singh. Conditional moment closure schemes for studying stochastic dynamics of genetic circuits. *IEEE Transactions on Biomedical Systems and Circuits*, 9:518–526, 2015.

[51] Mohammad Soltani and Abhyudai Singh. Effects of cell-cycle-dependent expression on random fluctuations in protein levels. *Royal Society Open Science*, 3:160578, 2016.

[52] Mohammad Soltani and Abhyudai Singh. Moment dynamics for linear time-triggered stochastic hybrid systems. *IEEE 55th Conference on Decision and Control*, pages 3702–3707, 2016.

[53] Mohammad Soltani and Abhyudai Singh. Moment-based analysis of stochastic hybrid systems with renewal transitions. *Automatica*, 84:62–69, 2017.

[54] Mohammad Soltani and Abhyudai Singh. Stochastic analysis of linear time-invariant systems with renewal transitions. In *American Control Conference*, pages 1734–1739, 2017.

[55] Mohammad Soltani and Abhyudai Singh. Linear piecewise-deterministic markov processes with families of random discrete events. *To appear in European Control Conference*, 2018.

[56] Mohammad Soltani, Cesar A Vargas-Garcia, Duarte Antunes, and Abhyudai Singh. Intercellular variability in protein levels from stochastic expression and noisy cell cycle processes. *PLoS computational biology*, 12(8):e1004972, 2016.

[57] David G Spiller, Christopher D Wood, David A Rand, and Michael RH White. Measurement of single-cell dynamics. *Nature*, 465(7299):736, 2010.

[58] Mukhtar Ullah and Olaf Wolkenhauer. Investigating the two-moment characterisation of subcellular biochemical networks. *Journal of Theoretical Biology*, 260:340–352, 2009.

[59] Nicolaas Godfried Van Kampen. *Stochastic Processes in Physics and Chemistry*, volume 1. Elsevier, 1992.

[60] César Augusto Vargas-García, Mohammad Soltani, and Abhyudai Singh. Conditions for cell size homeostasis: A stochastic hybrid systems approach. *IEEE Life Sciences Letters*, 2:47–50, 2016.

[61] Jan-Willem Veening, Wiep Klass Smits, and Oscar P Kuipers. Bistability, epigenetics, and bet-hedging in bacteria. *Annual Review of Microbiology*, 62:193–210, 2008.

[62] Ji Yu, Jie Xiao, Xiaojia Ren, Kaiqin Lao, and X. Sunney Xie. Probing gene expression in live cells, one protein molecule at a time. *Science*, 311:1600–1603, 2006.

[63] Gene-Wei Li Huiyi Chen1 Mohan Babu Jeremy Hearn Andrew Emili X. Sunney Xie Yuichi Taniguchi1, Paul J. Choi. Quantifying E. coli proteome and transcriptome with single-molecule sensitivity in single cells. *Science*, 329:533–538, 2010.